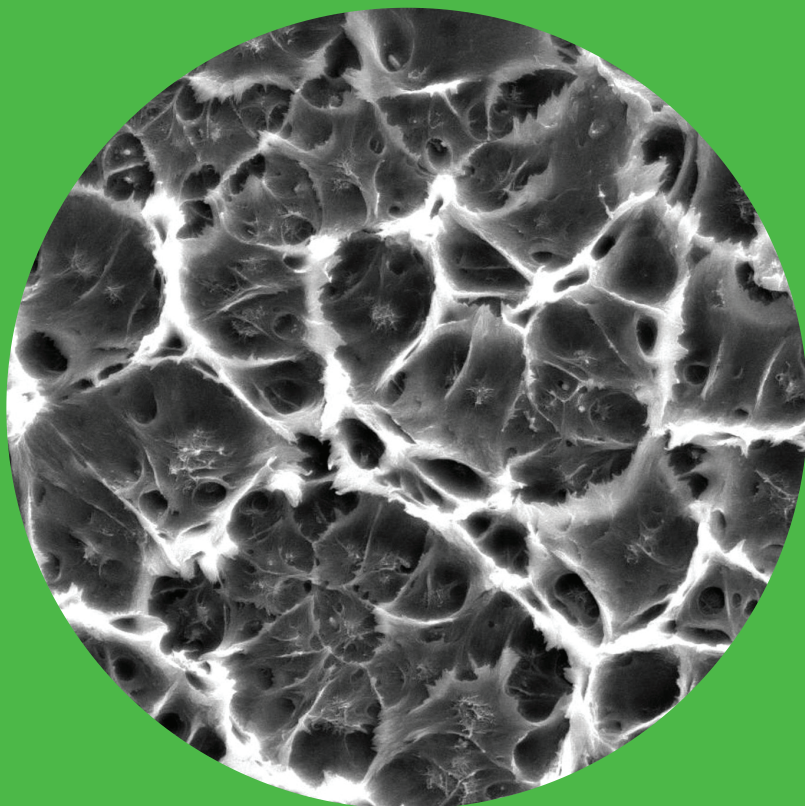


Department of Biotechnology and Chemical Technology

Electrically conductive polymeric materials through polymerization and compatibilization

Minna Annala



Electrically conductive polymeric materials through polymerization and compatibilization

Minna Annala

Doctoral dissertation for the degree of Doctor of Science in Technology to be presented with due permission of the School of Chemical Technology for public examination and debate in Auditorium (Forest Products Building 2) at the Aalto University School of Chemical Technology (Espoo, Finland) on the 2nd of November, 2012, at 12 noon.

Aalto University
School of Chemical Technology
Department of Biotechnology and Chemical Technology
Polymer Technology

Supervising professor

Jukka Seppälä

Thesis advisor

Professor Jukka Seppälä

Preliminary examiners

Professor Jae-Do Nam, Sungkyunkwan University, Korea

Doctor Jan-Erik Österholm, Fortum Oyj, Finland

Opponent

Professor Matti Elomaa, Tallinn University of Technology, Estonia

Aalto University publication series

DOCTORAL DISSERTATIONS 116/2012

© Minna Annala

ISBN 978-952-60-4780-5 (printed)

ISBN 978-952-60-4781-2 (pdf)

ISSN-L 1799-4934

ISSN 1799-4934 (printed)

ISSN 1799-4942 (pdf)

<http://urn.fi/URN:ISBN:978-952-60-4781-2>

Unigrafia Oy

Helsinki 2012

Finland

Publication orders (printed book):

Aalto University School of Chemical Technology,

Department of Biotechnology and Chemical Technology



Author

Minna Annala

Name of the doctoral dissertation

Electrically conductive polymeric materials through polymerization and compatibilization

Publisher School of Chemical Technology

Unit Department of Biotechnology and Chemical Technology

Series Aalto University publication series DOCTORAL DISSERTATIONS 116/2012

Field of research Polymer Technology

Manuscript submitted 7 March 2012

Date of the defence 2 November 2012

Permission to publish granted (date) 29 August 2012

Language English

Monograph

Article dissertation (summary + original articles)

Abstract

Three different electrically conductive polymeric materials were studied. In the first part, carbon nanotube (CNT) composites were prepared by using in situ polymerization of styrene and methyl methacrylate. Emulsion polymerization and combined emulsion/suspension polymerization methods were used. The mechanical properties of composites were improved directly due to the addition of the CNTs, but also indirectly due to the effect of CNTs on molecular weight and molecular weight distribution. The molecular weights increased and distribution narrowed, if CNTs were present in the polymerization reaction. The composites were conductive if the amount of CNTs was over 1.5 wt.% in polystyrene composites and over 3 wt.% in poly(methyl methacrylate) composites. As the stable dispersion of CNTs in the composites was obtained, these composites were tested as masterbatches.

In the second part, polyaniline (PANI) complex and polyethylene were blended to create an electrically conductive polymer blend. The PANI complex was plasticized in order to use melt blending and processing, and metallocene polymerization was utilized to prepare carboxyl acid and hydroxyl functionalized polyethylenes for compatibilization of the blend components. Compatibilization was based on hydrogen bonds, which do not decrease the conductivity of PANI to the same extent as covalent bonds. The polyethylene contained only 0.2 mol-% of functionalities. Therefore the number of formed hydrogen bonds was small. Conductivity above 10⁻⁴ S/cm was obtained with 15 wt.% of the camphorsulfonic acid doped PANI complex. The mechanical properties of the blend were clearly improved with addition of 18 wt.% of functionalized polyethylene.

In the third part, metallocene polymerization was utilized to prepare an ethylene/styrene copolymer, which was sulfonated in order to get a proton conductive polymer membrane. With the alternating structure of the copolymer with nearly 1:1 molar ratio of ethylene/styrene, sulfonic groups were evenly distributed along the membrane that was hot pressed from the copolymer. A high sulfonation degree with styrene content of 50 mol-% caused high water uptake and ion exchange capacity, thereby achieving high proton conductivity, above 70 mS/cm. Mechanical stability of highly sulfonated proton conductive membranes was improved by using a glassfiber tissue as reinforcement and by adjusting sulfonation conditions for crosslinking.

Keywords blends, nanocomposites, carbon nanotubes, compatibilization, conductivity

ISBN (printed) 978-952-60-4780-5

ISBN (pdf) 978-952-60-4781-2

ISSN-L 1799-4934

ISSN (printed) 1799-4934

ISSN (pdf) 1799-4942

Location of publisher Espoo

Location of printing Helsinki

Year 2012

Pages 140

urn <http://urn.fi/URN:ISBN:978-952-60-4781-2>

Tekijä

Minna Annala

Väitöskirjan nimi

Polymeroinnin ja kompatibilisoinnin avulla saadut sähköä johtavat polymeerimateriaalit

Julkaisija Kemian tekniikan korkeakoulu**Yksikkö** Biotekniikan ja kemian tekniikan laitos**Sarja** Aalto University publication series DOCTORAL DISSERTATIONS 116/2012**Tutkimusala** Polymeeritekologia**Käsikirjoituksen pvm** 07.03.2012**Väitöspäivä** 02.11.2012**Julkaisuluvan myöntämispäivä** 29.08.2012**Kieli** Englanti **Monografia** **Yhdistelmäväitöskirja (yhteenveto-osa + erillisartikkelit)****Tiivistelmä**

Työssä tutkittiin kolmea erilaista sähköä johtavaa polymeerimateriaalia. Ensimmäisessä osassa valmistettiin in situ -polymeroimalla komposiitit hiilen nanoputkista ja polystyreenistä ja poly(metyylimetakrylaattista). Polymerointitekniikkoina käytettiin emulsiopolymerointia ja yhdistettyä emulsiio/suspensio -polymerointia. Komposiitin mekaanisten ominaisuuksien parantuminen johtui suoraan hiilen nanoputkien lisäyksestä, mutta myös epäsuorasti, sillä hiilen nanoputkien läsnäolo polymerointireaktiossa kasvatti moolimassaa ja kavensi moolimassajakaamaa. Korkeamman moolimassan omaavalla polymeerillä on paremmat mekaaniset ominaisuudet verrattuna pienempi moolimassaiseen polymeeriin. Komposiitti oli sähköä johtava, kun polystyreeni-komposiitissa oli yli 1,5 m-% hiilin nanoputkia ja poly(metyylimetakrylaatti)-komposiitissa yli 3 m-% hiilen nanoputkia. Koska in situ -polymeroinnilla saatiin aikaiseksi stabiili hiilen nanoputkien dispersio, komposiitteja käytettiin myös masterbatcheina.

Toisessa osassa valmistettiin sähköä johtava polyaniliini-kompleksin (PANI) ja polyeteenin seos. PANI-kompleksi plastisoitiin, jotta sulaseostus ja -työstö olisivat mahdollisia, ja metallosemi-polymeroinnilla valmistettuja karboksyylihappo- ja hydroksyyli-funktionaalisia polyeteenejä hyödynnettiin kompatibilisaattoreina seoskomponenttien välillä. Kompatibilisointi perustui vetysidoksiin PANI-kompleksin ja funktionaalisen polyetyleenin välillä, sillä kovalenttiset sidokset voivat huonontaa PANI-kompleksin johtavuutta. Kompatibilisaattorina käytetty polyeteeni sisälsi ainoastaan 0,2 mol-% funktionaalisia ryhmiä, jolloin muodostuneiden vetysidosten määrä ei ollut suuri. Yli 10-4 S/cm johtavuus saavutettiin, kun seoksessa oli 15 m-% kamferisulfonihapolla dopattua PANI-kompleksia. Seoksen mekaaniset ominaisuudet paranivat selvästi, kun seokseen oli lisätty 18 m-% funtionaalista polyeteeniä kompatibilisaattoriksi.

Kolmannessa osassa metallosemi-polymeroitua eteeni/styreeni kopolymeeriä hyödynnettiin muodostamaan sulatyöstetty protonijohtava membraani. Kopolymeeri saatiin protonijohtavaksi sulfonoimalla styreeni-ryhmät. Koska kopolymeerin eteeni/styreenijärjestys oli lähes vuorotteleva, sulfonihappo-ryhmät olivat tasaisesti jakautuneet koko membraaniin, ja styreeni-pitoisuuden ollessa lähes 50 mol-% membraaniin ei muodostunut isoja polyeteeni tai polystyreeni-lohkoja. Suuren styreeni-pitoisuuden johdosta sulfonointiaste oli korkea ja membraanin veden ottokyky ja ioninvaihtokapasiteetti olivat suuret. Näiden johdosta saavutettiin myös hyvä protonijohtavuus, yli 70 mS/cm. Membraanin mekaanista stabiilisuutta parannettiin lasikuitumaton ja sulfonointireaktiossa tapahtuvan ristisilloituksen avulla.

Avainsanat seokset, nanokomposiitit, hiilen nanoputket, kompatibilisointi, johtavuus**ISBN (painettu)** 978-952-60-4780-5**ISBN (pdf)** 978-952-60-4781-2**ISSN-L** 1799-4934**ISSN (painettu)** 1799-4934**ISSN (pdf)** 1799-4942**Julkaisupaikka** Espoo**Painopaikka** Helsinki**Vuosi** 2012**Sivumäärä** 140**urn** <http://urn.fi/URN:ISBN:978-952-60-4781-2>

Preface

This work was carried out in the Polymer Research Group at Aalto University School of Chemical Technology (Helsinki University of Technology until January 2010). Financial support from the Academy of Finland and Tekes (the Finnish Funding Agency for Technology and Innovation) is deeply appreciated.

I wish to express my gratitude to my supervisor, Professor Jukka Seppälä, for the opportunity to work in his research group and for his interest in my research topic. I want to thank Dr. Barbro Löfgren and Dr. Ulla Hippo for their guidance and support through the years.

I would like to thank Heli Funck for her help and support for the PANI research and for being an out-of-lab-world-person for me. I would like to thank Dr. Mika Lahelin for his co-operation with the carbon nanotube research and Dr. Sami Lipponen for his overall practical help as well as for producing polymers. I would like to thank Dr. Tanja Kallio for her interest and help with proton-conducting materials. I would also like to express my gratitude to Dr. Jaana Rich for listening joys and sorrows and to the whole laboratory group for creating a nice working atmosphere.

Finally, I would like to express my warmest gratitude to my family and friends for all the support they have given to me during all these years.

Contents

LIST OF PUBLICATIONS

ABBREVIATIONS AND SYMBOLS

| | |
|---|-----------|
| 1. INTRODUCTION | 14 |
| 1.1 Background | 14 |
| 1.2 Conductive polymer composites | 15 |
| 1.2.1 Carbon nanotubes | 16 |
| 1.2.2 Functionalization of carbon nanotubes | 18 |
| 1.2.3 Dispersion of CNTs in the composites | 19 |
| 1.3 Intrinsically conductive polymers | 21 |
| 1.3.1 Doping and plasticizing of polyaniline | 23 |
| 1.3.2 Blending with other polymers | 25 |
| 1.4 Ionically conductive polymers | 25 |
| 1.4.1 Proton conductive polymer membranes | 26 |
| 1.5 The scope of the thesis | 28 |
| 2. CARBON NANOTUBE COMPOSITES | 30 |
| 2.1 The achievements in dispersing carbon nanotubes in polymers | 30 |
| 2.2 <i>In situ</i> polymerizations and processing | 31 |
| 2.2.1 Emulsion and suspension polymerization methods | 31 |
| 2.2.2 Materials and methods | 32 |
| 2.3 The effect of CNTs on the properties of the composites | 34 |
| 2.3.1 Molecular weight and molecular weight distribution | 34 |
| 2.3.2 Emulsion properties | 38 |
| 2.3.3 Composite properties | 41 |
| 2.4 The use of CNT composite as a masterbatch | 45 |
| 3. POLYANILINE BLENDS PRODUCED BY MELT MIXING | 51 |
| 3.1 The achievements in blending polyaniline with other polymers | 51 |
| 3.2 Materials and processing | 54 |
| 3.3 Conductivity of PANI blends | 56 |

| | | |
|-----------|---|-----------|
| 3.4 | Thermal Properties | 57 |
| 3.5 | Mechanical Properties | 58 |
| 3.6 | Morphology of PANI blends | 59 |
| 4. | PROTON CONDUCTIVE POLY(ETHYLENE-CO-STYRENE) MEMBRANES | 61 |
| 4.1 | The benefit of using metallocene polymers as a proton conductive material | 61 |
| 4.2 | Material preparations and characterizations | 62 |
| 4.3 | Structure and morphology of copolymer and membranes | 63 |
| 4.4 | Effect of sulfonation | 64 |
| 4.4.1 | Ion exchange capacity | 64 |
| 4.4.2 | Proton conductivity | 66 |
| 4.4.3 | Strength of membranes | 67 |
| 5. | CONCLUSIONS | 68 |
| | REFERENCES | 70 |

List of Publications

This thesis consists of an overview and the following publications which are referred to in the text by their Roman numerals.

- I Annala, M., Lahelin, M., Seppälä, J., The effect of MWCNTs on molecular mass in *in situ* polymerization of styrene and methyl methacrylate, *Eur. Polym. J.* **48** (2012) 1516-1524.
- II Lahelin, M., Annala, M., Nykänen, A., Ruokolainen, J., Seppälä, J., *In situ* polymerized nanocomposites: Polystyrene/CNT and poly(methyl methacrylate)/CNT composites, *Compos. Sci. Tech.* **71** (2011) 900-907.
- III Annala, M., Lahelin, M., Seppälä, J., Utilization of poly(methyl methacrylate) – carbon nanotube and polystyrene – carbon nanotube *in situ* polymerized composites as masterbatches for melt mixing, *Express Polymer Letters* **6** (2012) 814-825.
- IV Annala, M., Löfgren, B., Compatibilization of conductive polyethylene/polyaniline blends, *Macromol. Mater. Eng.* **291** (2006) 848-857.
- V Annala, M., Lipponen, S., Kallio, T., Seppälä, J., Proton conductive reinforced poly(ethylene-co-styrene) membranes, *J. Appl. Polym. Sci.* **124** (2012) 1511-1519.

The author's contribution to the appended publications

- I Minna Annala planned and carried out the polymerizations and characterizations of polystyrene-based composites and wrote the manuscript with the assistance of the co-authors.
- II Minna Annala planned and carried out the polymerizations and characterizations of polystyrene-based composites (excluding electron microscopy and dynamic mechanical analysis) and contributed to preparation of the manuscript.

- III** Minna Annala planned and carried out the experiments (excluding polymerization of poly(methyl methacrylate)) and wrote the manuscript with the assistance of the co-authors.

- IV** Minna Annala planned and carried out the experiments (excluding polymerization of functionalized polyethylenes and NMR measurements) and wrote the manuscript with the assistance of the co-authors.

- V** Minna Annala planned and carried out the experiments (excluding the polymerization of ethylene/styrene copolymer, NMR, and a.c. conductivity measurements), and wrote the manuscript with the assistance of the co-authors.

Abbreviations and Symbols

| | |
|----------------|---|
| ϕ | volume fraction |
| Ω | electrical resistance |
| α | constant of system dimension |
| γ_N | nominal strain |
| $\dot{\gamma}$ | shear rate |
| δ_f | tensile strength of fiber |
| η | viscosity |
| σ | conductivity |
| τ_c | fiber-matrix bond strength |
| d | fiber diameter |
| k | number of different screw speeds |
| t | time |
| AIBN | azobisisobutyronitrile |
| CNT | carbon nanotube |
| COOH | carbocyclic acid functionality |
| CSA | camphorsulfonic acid |
| DBSA | sodium dodecyl benzene sulfate, dodecyl benzene sulfonic acid |
| DCE | dichloroethane |
| DLS | dynamic light scattering |
| DMA | dynamic mechanical analysis |
| DSC | differential scanning calorimetry |
| EMI | electromagnetic interference |
| ESD | electrostatic discharge |
| EVA | ethylene/vinyl acetate copolymer |
| IEC | ion exchange capacity |
| KPS | potassium peroxydisulfate |
| LDPE | low density polyethylene |
| LED | light emitting device |
| MAH | maleic anhydride |
| MMA | methyl methacrylate |
| M_w | molecular weight [g/mol] |
| MWCNT | multi-walled carbon nanotube |
| N | rotation speed |
| NMR | nuclear magnetic resonance |
| OH | hydroxyl functionality |

| | |
|-------------------|------------------------------------|
| PANI | polyaniline |
| PD | polydispersity of molecular weight |
| PE | polyethylene |
| PMMA | poly(methyl methacrylate) |
| PS | polystyrene |
| PSA | phenolsulfonic acid |
| PVDF | poly(vinylidene fluoride) |
| SDS | sodium dodecyl sulfate |
| SEC | size exclusion chromatography |
| SEM | scanning electron microscopy |
| SO ₃ H | sulfonic acid group |
| TEM | transmission electron microscopy |
| T | temperature |
| T ₀ | Mott characteristic temperature |
| T _g | glass transition temperature |
| TSA | toluenesulfonic acid |

1. Introduction

1.1 Background

Traditionally, polymers are counted as insulators. The properties of polymers are, however, beneficial in respect of materials for conductive applications. Polymers are mostly easy to process and recycle. Compared with most metals, polymers are resistant to corrosion. Due to the possibility of tailoring the density and porosity, polymer-based applications are lightweight and the prices are lower in comparison with most metals.

Based on these benefits of the polymers and the possibility to control the conductivity, polymers have been utilized in the applications where electrical conductivity is needed. [1-5] The electrical conductivity can be expressed as resistance (Ohm, Ω) or as conductance (Siemens, S), which is an inverse quantity of resistance. Depending on the specimen or the application, the conductivity can be expressed as surface or volume conductivity.

Based on the application field and desired properties, conductive polymeric materials can be divided into three categories. Two of these categories consist of polymeric materials having electronic conductivity. In the first category, electronic conductivity is formed by using a filled insulating polymer matrix with conductive particles such as metal or carbon black. [5] In the case of blends and composites, the term 'percolation threshold' is used to depict the transition from insulator to conductive material. In the late 1980s, intensive research focused on intrinsically conductive polymers, as polyaniline or polypyrrole, which form the second category. [6,7] Electronic conductivity is based on conjugated double bonds in the backbone of intrinsically conductive polymers. In addition to electronically conductive polymeric materials, ionically conductive polymer materials are required. Ionically conductive polymers form the third category of conductive polymeric materials. Ionic conductivity is usually formed by using sulfonic acid groups in the side chains of polymers and conductivity is most commonly based on protons. Therefore, ionic conductivity is often called proton conductivity. [8,9]

Conductivity is often divided into areas that are insulating, static dissipative, and conductive (Fig. 1). The conductivity level can be clear conductivity, above 10^{-3} S/cm, which is required for electromagnetic shielding (EMI-shielding), but often 10^{-6} – 10^{-5} S/cm is counted as a conductive material. This conductivity level is required to prevent electrostatic discharge (ESD). [4,5]

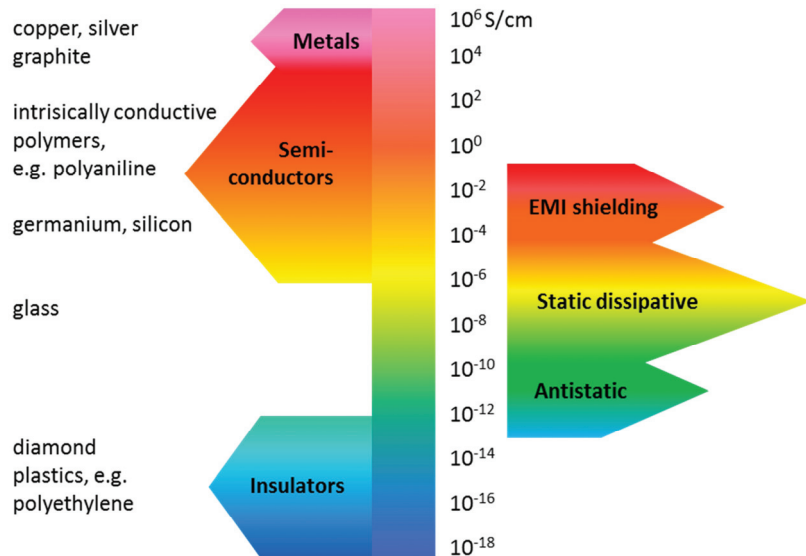


Figure 1. General conductivity levels and conductivities of different materials.

1.2 Conductive polymer composites

The most common way to produce conductive polymers is to compound metal or carbon based particles into a polymer matrix. [5] To be a conductive composite, added particles must form continuous paths through the polymer matrix, and controlling these paths is a major challenge. When inexpensive carbon black is used to make conductive composite, the amount of carbon black can be high, exceeding the theoretical percolation threshold of 16 vol-%, [10] and there is no need to put a lot of effort creating specific percolation morphologies within the composites. [11,12] However, usually there is a need to minimize the filler content in the composite. By using solution processing, it is easier to minimize the amount of conductive component and at the same time to control the morphology of the composite. Solution processing has been used to prepare specific morphologies in conductive composites. The amount of conductive component has been successfully decreased below 0.2 wt.%, yet

maintaining high conductivity of the composite. [13,14] Industrial processing scale, however, prefers melt processing and application areas consist of electrostatic dissipation or electromagnetic shielding with higher amounts of conductive component.

At the same time, added conductive particles can improve the mechanical properties of the composite, provided that interactions between components are adequate. To improve adhesion between components, functional components, compatibilizers, could be added to the composite, or conductive particles could be functionalized. There is possibility, however, to decrease the conductivity of particles or even destroy it.

Because of the challenges in forming conductive composites by minimizing the amount of the conductive component, research and development on novel nanoparticles has enabled advanced composites to be made. In addition, nanoparticles have properties that are not present in their bulk materials. Nanosized silver particles have antibacterial properties, [15] and carbon nanoparticles, such as carbon nanotubes and graphene, have properties that can compete with copper or diamond. [16-18] The use of these types of nanoparticles in composites is aimed at carrying the unique properties of nanoparticles over the composite. Embedding nanoscale particles in polymers offers a means of producing multifunctional polymer composites with enhanced mechanical, electrical, optical, thermal, or magnetic properties.

The dispersion of nanoparticles, however, continues to remain a critical issue concerning nanocomposites. In order to benefit from using nanoparticles it is required that they are individually dispersed into the matrix. In agglomerated form, nanoparticles can be considered as microsized particles, and the benefit of the special properties derived from the nano size is lost as is the possibility to use minimal amount of nanofiller. A conductive nanocomposite requires an even more specified dispersion morphology, as individual nanoparticles must be close enough for electrons to tunnel or hop from particle to particle through the polymer matrix. [19,20] In recent years, carbon nanotubes (CNTs) have become the most studied nanomaterials in conductive composites.

1.2.1 Carbon nanotubes

Carbon nanotubes (CNTs) are unique materials with superior mechanical, thermal, and electrical properties. [16-18] A CNT can be depicted as a

graphene sheet that has been rolled into a tube. The tube can comprise one or several rolled sheets, forming a single-walled carbon nanotube or a multi-walled carbon nanotube, respectively. The sheet can be rolled at different specific angles, expressed as chirality (Fig. 2). Based on the chirality of CNTs, conductivity can vary from semiconducting to metallic. The chirality can be expressed as a vector, C_h , specified by a pair of integers (n, m) . The structure of the CNTs is termed a zigzag when the vector is $(n, 0)$, and an armchair when the vector is (n, n) .

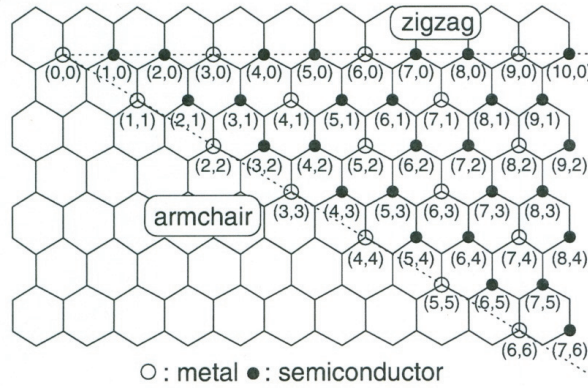


Figure 2. Chirality of carbon nanotubes. The carbon nanotubes that are metallic and semiconducting, respectively, are denoted by open and solid circles on the map of chiral vectors (n, m) . All possible chiral vectors $C_h = na_1 + ma_2$ are specified by the pairs of integers (n, m) for general carbon nanotubes, including zigzag, armchair, and chiral nanotubes. Reprinted with kind permission from Springer Science and Business Media. [16] Copyright 1999 Springer-Verlag.

Even though the structure and conductivity of the CNTs can be determined, it is still not possible to control the structure of the CNTs and to prepare CNTs with a specific conductivity level, semiconducting or metallic. Therefore various CNTs are present, consisting semiconducting and metallic conductivities. Similarly, when CNTs are used in composites, the conductivity of the CNTs defines the highest conductivity that can be obtained in the composite.

CNTs have a high aspect ratio, i.e. a very small diameter in relation to the length. The aspect ratio of the CNTs can be over a thousand; therefore, the CNTs can be considered as fibers instead of particles in the matrix. A high aspect ratio provides the possibility of making organized structures in the composite. However, the high surface area increases bundling of the tubes, and the separation of individual CNTs (even in solvents, both water and organic solvents) has limited their practical use. [21] Owing to the high surface energy and strong van der Waals interactions, it is difficult to

disperse the CNTs in the polymer at the nanoscale level through simple mixing. A lot of effort has been focused on the functionalization of the CNTs to provide CNT agglomerates with improved solubility and dispersion. [22-25]

1.2.2 Functionalization of carbon nanotubes

Functional groups can be attached to the CNTs by forming covalent or non-covalent bonds. Covalent bonds can be formed at the ends or defect sites of a CNT, which is the most common method of functionalizing the CNTs. Often the first step of functionalization is the oxidation of the CNTs, in which hydroxyl or carboxylic groups are attached to the CNTs. [23,24] However, it has been proposed that the oxidation of the defect sites with nitric acid etches the CNTs. Carboxylated carbonaceous fragments can adsorb on the CNTs and the number of functional groups on the CNTs increases. [24] Due to the etching, it is possible to cut CNTs during oxidation. Therefore, multi-walled CNTs are more stable in functionalization reactions. Functionalization of the sidewall of the CNTs is more complex because the reactivity of the CNTs depends on the diameter of the tubes and how carbon atoms are organized in relation to each other, i.e. pyramidalization. [22] Functionalization of CNTs may, however, alter the chirality of CNTs and their conductivity. The conductivity of CNTs can, therefore, be decreased or even destroyed after functionalization, if functional groups are covalently attached to the surface of CNTs.

By using non-covalent functionalization, the conductivity of a CNT remains unaltered. Non-covalent functionalization is based on physical bonds, van der Waals forces or π - π stacking. In non-covalent functionalization, the CNTs are wrapped by using surfactants, polymers, and biomolecules, such as proteins. [25]

The functional groups attached to the CNTs provide the possibility to improve both the dispersion of the CNTs and the reinforcement of composites that contain functionalized CNTs. Based on the high aspect ratio, CNTs can be considered as fibers. In composites, the reinforcement of fibers depends on the length of the fibers and interactions between the fibers and a matrix. There is a critical fiber length that is necessary for the reinforcement of composites according to equation 1: [26]

$$\text{critical fiber length} = \frac{\delta_f \cdot d}{2\tau_c} \quad (1)$$

where d is the fiber diameter, δ_f is the tensile strength of the fiber, and τ_c is the fiber-matrix bond strength. Based on equation 1, functionalization of the CNTs affects the reinforcement effect as τ_c increases, and in consequence, critical fiber length can be shorter.

1.2.3 Dispersion of CNTs in the composites

The challenge of CNT composites has been to achieve nanodispersion of CNTs in the polymer composite, thus obtaining the desired combination of electrical conductivity and mechanical properties with the lowest possible CNT content. Research has been focused on obtaining homogeneous and fine dispersions of the CNTs in polymers by using conventional mixing techniques, *in situ* polymerization in the presence of nanotubes, and combinations of these techniques. [27-33]

Compromises have to be made in order to get good reinforcement and electrical conductivity in the resulting composite. The orientation of the CNTs in composites has contradictory effects on the properties of the composite. Well-aligned CNTs in the composite improve mechanical properties. [34,35] On the other hand, electrical conductivity decreases in well-aligned CNTs, as the electrical conductivity of the composites is based on the interpenetrating network of the conductive particles throughout the composite. [36-38] The percolation threshold depends on the matrix polymer, CNTs, and processing of the composite. [39,40]

With *in situ* polymerization, it is possible to simultaneously obtain a homogeneous dispersion and a strong interface between CNTs and a polymer matrix. Emulsion polymerization and related methods are some of the most effective polymerization techniques for preparing *in situ* polymerized CNT composites. [32,41-44] Vigorous sonication is normally used to break down CNT agglomerates before mixing with polymers or *in situ* polymerization. [45]

With conventional mixing in solution or in melt mixing, a stable nanoscale dispersion of the CNTs is difficult to achieve. [27] In solution mixing, initial dispersing of the CNTs is easier due to the possibility of using solvents that have enhanced interactions with the CNTs, and different mixing treatments, like ultrasound, are possible to adopt. However, the removal of solvent can induce the reagglomeration of nanoparticles. [46] In melt mixing, possibilities are only limited to the dispersion of CNTs. Dispersing of nanoparticles is based on the shear forces that are formed during melt

mixing. In the simple model for extrusion, the total shear strain applied on the sample during melt mixing can be affected by the mixing time and the rotation speed, since the screw speed is proportional to the shear rate, according to equation 2: [47]

$$\gamma_N = \sum_{i=1}^k \dot{\gamma}_i \cdot t_i \propto \sum_{i=1}^k N_i \cdot t_i \quad (2)$$

where γ_N is the nominal strain in the melt, $\dot{\gamma}$ is shear rate, t is time, N is rotation speed, i denotes the different screw speeds used during the mixing history, k is the number of different screw speeds used in the mixing history.

Direct melt mixing and the use of a masterbatch are yet the desired processing methods in many applications. The dispersion of the CNTs in a polypropylene matrix in melt mixing has been improved by using functionalized CNTs and a compatibilizer. [48] The mixing conditions in different melt mixers and the effect of shear on CNT agglomerates during mixing have been studied, and new concepts for direct melt mixing have been developed, such as an ultrasonic-assisted extruder. [28,29]

To use a masterbatch, the CNTs are first dispersed in one polymer and this composite is then melt blended or diluted with a second polymer. Though melt mixing is a reasonably economic way to produce a wide range of polymer blends, the control over blend morphology is more difficult compared with solution blending. Improvement in the mechanical properties of a blend requires that the phase of the polymer having better mechanical properties is continuous, and that there is sufficient adhesion between the phases. In melt mixing, phase separation can be controlled by adjusting the viscosity ratios and the shear rates to achieve a morphology in which both phases are continuous or the CNT-rich polymer phase is continuous. [47,49] In such blends, double percolation can be exploited to minimize the CNT content in the composite. [50,51] The phase morphology of the blend consisting of two polymers can be predicted according to equation 3: [49]

$$\frac{\eta_1}{\eta_2} \cdot \frac{\phi_2}{\phi_1} \cong 1 \quad (3)$$

where η is the viscosity and ϕ the volume fraction. Simultaneous interpenetrating networks of polymer phases are formed when the quantity is approximately unity. The phase of polymer 1 is continuous when the quantity is less than unity.

1.3 Intrinsically conductive polymers

Intrinsically conductive polymers have been studied intensively during recent decades. [5-7] The electrical conductivity is based on conjugated double bonds in the backbone with delocalized electrons through the chain of the polymers. For example, polyacetylene, polypyrrole, polythiophene, polyparaphenylene, polyaniline, and their derivatives are such polymers (Fig. 3). The benefit of intrinsically conductive polymers is that conductivity can be adjusted by doping. In doping, the amount of charge carriers increases through redox chemistry, and thus conductivity enhances. The applications of intrinsically conductive polymers can be related to the doping method. [7] With chemical doping, it is possible to affect the properties of a polymer, and applications include transparent electrodes, antistatics, and EMI-shielding (Fig. 1). With electrochemical doping, electrochemical potential can be controlled. Therefore the applications consist of electrochemical batteries and light-emitting electrochemical cells. With photodoping, optical materials can be produced for photovoltaic devices.

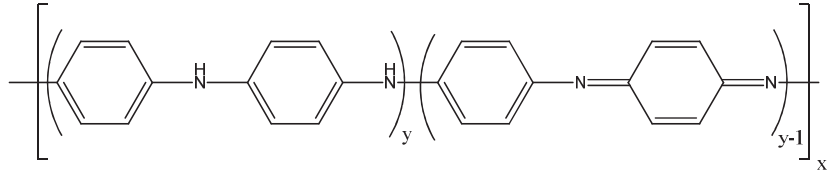


Figure 4. Different oxidation stages of polyaniline. Leucoemeraldine $y=1$, emeraldine $y=0.5$, and pernigraniline $y=0$.

1.3.1 Doping and plasticizing of polyaniline

The dopant can form hydrogen bonds or ionic bonds and van der Waals interactions with the PANI chain. In the case of PANI, it is possible to use acid-base chemistry for doping. The amount of electrons in the chain remains constant when the iminic nitrogen atoms are protonated with protonic acid, such as sulfonic acid. With other chemical doping methods, the amount of electrons increases when PANI is oxidized or reduced, depending on the oxidation state. [7,52,56]

In the protonated PANI chain, the charge carriers are solitons (cations), polarons (radical cations), and bipolarons (dications). At a low doping level there are mostly solitons in the chain. When doping level increases, the number of polarons and bipolarons increases. Proper conductivity is created when polarons or bipolarons are present in the PANI chain (Fig. 5). [7,57] Based on the movement of charge carriers, bulk conductivity consists of intramolecular, intermolecular, and interdomain conductivity. [6] The conductive mechanism in PANI is considered a three-dimensional or a one-dimensional variable-range-hopping model (VRH). There are some parallel coupled chains that are metallic bundles. The charge transport between these bundles is 1D VRH. Inside the bundles, electrons become delocalized and 3D VRH dominates. VRH can be expressed as in equation 4: [58-60]

$$\sigma = \sigma_0 \exp \left[- \left(\frac{T_0}{T} \right)^\alpha \right] \quad (4)$$

where T_0 is the Mott characteristic temperature and σ_0 the conductivity at $T = \infty$. T_0 and σ_0 are determined by the localization length, the density of states, and the hopping distance in the material. α is determined by the dimension of the system, for 1D VRH $\alpha = 1/2$ and for 3D VRH $\alpha = 1/4$. In addition, there can be crossovers in α between $1/2$ and $1/4$. [60] Both the doping level and the dopant affect α . 1D VRH dominates when PANI is heavily doped. [59] When a small dopant is used, 3D VRH dominates the bulk conductivity. [58]

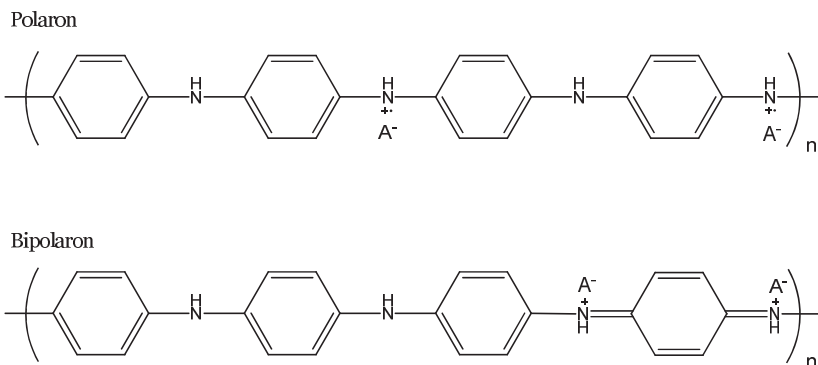


Figure 5. Charge carriers in the PANI chain, A^- is dopant anion.

In addition to primary doping, in which conductivity is enhanced by increasing charge carriers, there can be secondary doping and co-doping or over-doping. These other doping types enhance conductivity indirectly by changing the conformation of the molecule complex. Therefore, if the secondary dopant is removed, the obtained conductivity remains. In co-doping, both dopants can act as primary or secondary dopant. In over-doping, there is an excess of dopant that can act as plasticizing agent and affect the processing properties of PANI. [56,61,62]

PANI is usually doped with sulfonic acids, because the counterion part is larger than a small molecule acid such as hydrochloric acid. A large counterion can improve the delocalization of electrons by inhibiting the bending of the polymer chain and by increasing the distance between polymer chains when electrons are localized in one chain. Small counterions have a higher charge density and are able to form strong electrostatic interactions with nitrogen atoms in the PANI chain and hinder the delocalization of electrons along the chain. Dodecyl benzene sulfonic acid (DBSA), camphorsulfonic acid (CSA), and *p*-toluenesulfonic acid (TSA) are often used as dopants for PANI. [63]

Protonic acids can improve the processability of PANI, if the counterion part is functional and increases interactions with solvents or increases the thermal stability of PANI. The plasticizing effect is improved by using an excess amount of dopant. In addition, the plasticizing of PANI is enhanced by using other plasticizing agents that can be bonded with PANI through the molecular recognition of coordination bonds. [64,65]

1.3.2 Blending with other polymers

Although the addition of sulfonic acids as dopants causes intractable polyaniline to become soluble and, after plasticizing, can even be melted, the polyaniline complex still remains brittle. Therefore, PANI is blended with other polymers for improving mechanical properties. The blend morphology is even more important than in the conductive composites of CNT. The PANI phase must be continuous in order for the blend to be conductive. In addition, the improvement of the mechanical properties of a blend requires a continuous phase of the matrix polymer and sufficient adhesion between the phases. [66]

The research on PANI blends has mainly focused on solution blending, as it is then easier to control the morphology and minimize the PANI content. [61,67,68] In melt blending, phase separation can be controlled by adjusting the viscosity ratios and shear rates to achieve a morphology in which both phases are continuous, as in the preparation of carbon nanotube composites from a masterbatch according to equation 3. [49] Double percolation has been exploited to minimize the PANI content in the melt blend. For example, PANI complex is first solution blended with one polymer, and this blend is then melt blended with a second polymer. [69]

There are sufficient interactions between polar PANI and polar matrix polymers to keep the mechanical properties of the blend at the adequate level. However, the challenge is how to prepare a blend of PANI and non-polar matrix polymers, e.g. polyolefins. The use of common compatibilizers can destroy the conductivity of PANI when the compatibilizer reacts with the dopant.

1.4 Ionically conductive polymers

Polymers with ionic conductivity are gaining ground from traditional ionically conducting materials, as they are useful materials for ion exchange membranes, separators, sensors, and electrolytes in electrochemical cells. [8,70,71] Many polymeric electrolytes exhibit properties that other electrolytes are lacking, i.e. adequate ionic conductivity for practical purposes, low electronic conductivity, good mechanical properties, and chemical, electrochemical, and photochemical stability. In general, ionically conductive polymers have negatively or positively charged groups attached to a backbone or side chains by covalent bonds, and conductivity is based

on ions that are transported through the polymer. Therefore, a medium for transportation is normally needed.

Conductivity is often based on protons, and polymers with ionizing groups can be divided into two categories: sulfonated polymers and blends of polymers with oxoacids. [70-72] The usual functionality is a sulfonic acid group, SO_3^- , which can be covalently bonded to the side chain, as in most fluoropolymers, or directly to the backbone, as in most phenolic polymers. With negatively charged sulfonic acid group, the used medium is water or humidified vapors, which limit the operating temperature in the applications. Water is also used as medium with the polymers containing amino and amine groups in the backbone. However, the benefit with these polymers is that they can be used with other media as well. Heterocycles, such as imidazole and pyrazole-based polymers with phosphoric acid, have better thermal stability compared with most of the sulfonated polymers. [73,74] Without a water-based medium, these polymers can be proton conductive above 100 °C.

Proton conductivity is based on the diffusion of protons through the polymer. There are two main diffusion mechanisms in sulfonated polymers. In vehicle diffusion, protons migrate as hydronium ions. Therefore, the mobility of protons is dependent of water molecules. In structure diffusion (proton hopping, Grotthuss mechanism), protons jump along the hydrogen bonds formed by hydronium ions and water molecules. The bulk conductivity in sulfonated polymers is the combination of both diffusion mechanisms. [8,75-77] In imidazole-based polymers, the proton diffusion occurs mainly by the structure mechanism. [78]

1.4.1 Proton conductive polymer membranes

One ionomer of interest is a proton-conducting polymer membrane, where ionic conductivity is caused by hydrogen ions. Proton-conducting polymer membranes are mostly prepared by adding sulfonic acid groups to the hydrophobic backbone, where hydrophilic sulfonic acid groups create paths for proton transportation and the hydrophobic part of the polymer provides mechanical strength for the membrane. Proton-conducting polymer membranes have been used as actuators and sensors, electron-injecting and hole-blocking material in LEDs, and electrolytes in fuel cells. [71,79-85]

Sulfonated polystyrene is the mostly used proton-conducting ionomer in ion exchange applications. [86] Highly sulfonated polystyrene exhibits good

proton conductivity. However, it becomes water-soluble as the sulfonation degree increases. A better chemical stability and a high proton conductivity are achieved when perfluorinated or partially perfluorinated polymer membranes are radiation grafted with styrene and subsequently sulfonated. [9,70] Nafion, a sulfonated tetrafluoroethylene manufactured by DuPont, is the most common membrane used in the fuel cell, where the requirements for the membranes are demanding regarding proton conductivity and mechanical, barrier, and thermal properties.

In sulfonated membranes, water is a transport medium for protons. The amount of water in membranes affects both conductivity and mechanical properties. As the diffusion of protons through a membrane can occur by vehicle and hopping mechanisms, the state of water affects conductivity. It has been observed that there are three different states, in which water can occur: free water, loosely bound water, and bound water. [72,87,88] The first hydration shell around sulfonic acid groups is formed by the bound water molecules. There is proton transfer from sulfonic acid groups to water. The bound water is not able to crystallize, i.e. is non-freezing water. The second hydration shell is formed by loosely bound water molecules that are interacting with sulfonic acid groups, but they are able to crystallize, i.e. they are freezing bound water. Water molecules without interaction with sulfonic acid groups are free water or bulk water with dynamics similar to that of liquid water. The state of water depends on the amount of water and the number of sulfonic acid groups present. With less than nine water molecules per sulfonic acid group, i.e. hydration level under 9, there is mainly bound water in the membrane. By increasing hydration level above 9 there is additional loosely bound and free water in the membrane. The sulfonic acid groups with surrounded water shells form clusters that are connected together by free water, creating proton conductive paths in the membrane. Therefore, good proton conductivity requires the presence of both loosely bound and free water in the membrane. Many large water channels, however, may weaken the mechanical properties of the membrane.

The weak mechanical properties of proton-conducting membranes are usually caused by high water uptake leading to the swelling of membranes. It is possible to affect the water uptake by controlling the water channels in the membranes, as the formation of the water channels is based on the phase separation of hydrophobic and hydrophilic segments. Sulfonic acid groups attached to the ends of long side chains rather than to the backbone of an ionomer yield better phase separation, because the mobility of

sulfonic acid groups is higher. [77] Therefore, the mechanical properties of the membranes can be affected by tailoring the ionomer. Provided that the hydrophilicity of the membranes is high, crosslinking and reinforcement can be used to improve the mechanical properties. [89-92] Hydrophilicity of sulfonated polystyrene has been reduced by adding hydrophobic blocks to the backbone of polystyrene. Due to the hydrophobic blocks, phase separation is stronger in the membrane and the mechanical properties were improved. [93-97] In general, the hydrophobic blocks stabilize the ionomer, and the sulfonic acid groups form cluster networks for protons to diffuse in block copolymers. [98] The copolymer polystyrenesulfonate-*block*-polymethylbutylene (PSS-*b*-PMB) was more effective in retaining water with improved proton conductivity at elevated temperatures, if the hydrophilic domains had been reduced to less than 6 nm in width. [99] The same idea is exploited in polymer blends, where one blend component acts as an ionomer. [100,101] In block copolymers and polymer blends, mechanical and conducting properties can be improved by modifying the morphology of the membrane and restricting the swelling of the hydrophilic part.

1.5 The scope of the thesis

A great deal of work has been done in preparing electrically conductive polymeric materials. Unsolved issues, however, still remain concerning good conductivity with good mechanical properties. The aim of the thesis was to study electrically conductive polymer materials and the effects of polymer modifications through polymerization and compatibilization in order to improve the conductivity and mechanical properties of these materials. The emphasis was in melt processing and melt processable materials, as melt processing is a more economical way to produce products.

With polymers produced by utilizing advanced polymer synthesis or by using more conventional polymerization techniques, similar approaches can be used despite the different types of conductivity systems. The thesis summarizes the three different conductivity systems that were studied. Carbon nanotubes were utilized to form electronically conductive nanocomposites (publications I-III). The aim with carbon nanotube composites was to form a stable dispersion of individual carbon nanotubes in the polymer matrices with improved electrical and mechanical properties by using *in situ* polymerization techniques and double percolation theory. The studies showed that CNTs affect the molecular weight and molecular

weight distribution of polystyrene and poly(methyl methacrylate) when different *in situ* emulsion and suspension polymerizations techniques, surfactants, and CNT types were used. By using *in situ* polymerization, stable dispersions of CNTs were formed, which made it possible to use these composites as masterbatches. The viscosities of the *in situ* polymerized masterbatches were tailored to form conductive paths in the final composites and improve the conductivity of the final composite.

Double percolation was utilized to form an electronically conductive polymer blend based on polyaniline and polyolefins (publication IV), where PANI provides the conductivity and a polyolefin the mechanical stability for the blend. The primary aim of this study was to investigate the use of functionalized polyethylene and polypropylene as compatibilizers between PANI and a polymer matrix in melt processing. The compatibilization is based on hydrogen bonding between the PANI complex and functionalized polyethylene, as the covalent bonds have a tendency to destroy the conductivity of PANI.

The possibility to use functionalized polyolefins in proton-conducting membranes was studied in order to find a replacement for fluorine containing polymers or a highly protonated polymer that is water soluble (publication V). Using metallocene catalysts, ethylene/styrene copolymers were prepared and sulfonated. As the molar ratio of ethylene/styrene copolymer was almost equal, the conductivity was high, but at the same time, the swelling increased due to increased water uptake. Therefore, the glassfiber tissue was used to support the membrane structure for the highly sulfonated copolymer.

2. Carbon nanotube composites^{I-III}

2.1 The achievements in dispersing carbon nanotubes in polymers

In general, meeting the challenge of controlling and predicting nanocomposite properties requires an understanding of interfacial phenomena between the particles and polymers. Improved electrical conductivity is perhaps the most promising application area for CNTs at the moment. If CNTs are efficiently dispersed and yet percolate, a very small amount of CNTs can bring good electrical conductivity on otherwise insulating polymers. Embedding of CNTs in thermosets is relatively easy when solution processing can be applied. A low percolation threshold has been obtained, even as low as 0.001 wt.% of CNTs in epoxy. [14] The challenge is to embed CNTs in thermoplastics that have a higher molecular weight. Therefore, the processing of thermoplastics is more difficult. Solution processing needs specific solvents and melt processing is even more complex when good dispersion of CNTs is required.

Molecular weight and crystallinity of the polymer affect the mechanical and thermal properties. It has been observed that nanotubes act as nucleating agents and thus increase the crystallization temperature, the rate constant of crystallization, and the dimensions of the crystallite growth of polypropylene. [102] The thermodynamically driven migration effect can be used to obtain well-dispersed CNTs in a polymer matrix. When a polyethylene-CNT masterbatch was used in extrusion with polycarbonate or polyamide, the CNTs migrated into matrix polymers that had lower interfacial energies with the CNTs. [103] The percolation threshold was achieved at a lower CNT content than that needed with the direct incorporation of the CNTs. The CNTs can reorganize during melt mixing and the viscosity of the polymer determines to what extent the CNTs can reorganize because it determines their diffusivity. [104]

In situ polymerization techniques have been used to disperse CNTs individually into polymers. [32,41-44] In *in situ* polymerization, good dispersion of CNTs can be maintained without the problems that are faced in solution and melt processing. In solution processing, slow evaporation of

solvent enables the reagglomeration of CNTs. [27] In melt processing, there are hardly enough shear forces to break the agglomerates of CNT. However, there are only a few studies on how the polymer affects the properties of the CNT composites or how CNTs are involved in the *in situ* polymerization reactions. It has been observed that a broad molecular weight distribution decreased the percolation threshold in PS/CNTs and PMMA/CNTs composites that were solution processed. [13] The focus in the research on preparing CNT composites was therefore on the molecular weight of a matrix polymer prepared by using an *in situ* polymerization technique.

2.2 *In situ* polymerizations and processing

Owing to the high tendency of bundling, CNTs are usually exposed to strong ultrasound treatments in terms of time and power often exceeding 600 W. The treatment breaks up CNT bundles but also damages CNTs. A milder ultrasound treatment before polymerization was used in order to prevent the breaking of CNTs, and *in situ* polymerization was used to stabilize the dispersion after ultrasound treatment. For stabilization purposes, two polymerization techniques were tested: emulsion polymerization and combined emulsion/suspension polymerization.

2.2.1 Emulsion and suspension polymerization methods

Emulsion polymerization is a free-radical chain polymerization in a heterogeneous system. The monomer, surfactant, and dispersing medium, typically water, form a stable two-phase system. The weight ratio of water to monomer is 70/30 to 40/60. The initiator is water-soluble and radicals are formed in the aqueous phase. There is a critical concentration of surfactant, which must be exceeded in order to form surfactant micelles in the water. In micellar nucleation, polymerization can start in the micelles when the radicals enter the monomer-swollen micelles. In homogeneous nucleation, polymerization starts in the aqueous phase and water-soluble oligomeric radicals are formed. After the oligomeric radicals reach the limit of their solubility, they precipitate out of solution and form primary particles that adsorb surfactant. In droplet nucleation, radicals enter monomer droplets and propagate to form particles. [105,106]

The progress of polymerization can be divided into three intervals based on the number of particles. In the first interval, the number of particles increases with time. In the second and third intervals the number of

particles remains constant. In the third interval, monomer droplets are no longer present. [105,106]

The advantage of emulsion polymerization is that with emulsion polymerization it is possible to obtain both high molecular weights and high reaction rates. Due to the emulsion form, viscosity and heat transfer can be controlled easily. The product, latex, can be used directly in paintings, coatings, and adhesives without further separations. [105,106]

In suspension polymerization, the initiator is water-insoluble. Therefore, the initiator is dissolved in the monomer and the solution is suspended in the aqueous phase. The weight ratio of water to monomer is usually 1:1 to 4:1. In suspension polymerization, the amount of surfactant is much smaller in comparison with emulsion polymerization and the two-phase system is maintained by continuous agitation. Due to the small amount of surfactant, the monomer droplets are larger in suspension polymerization than in emulsion polymerization. Polymerization occurs in the monomer droplets, which can be considered as bulk polymerization in a very small scale and normal homogeneous free-radical polymerization kinetics apply. Because of the large particles, the product can be used in dried form, after the removal of surfactants. [105]

Based on the ability to disperse CNTs in the emulsion before the addition of monomers and initiators and the possibility to maintain the dispersion of CNTs, emulsion polymerization was chosen as one polymerization method. On the other hand, suspension polymerization was interesting due to the different polymerization kinetics and the possibility to disperse CNTs. Due to the requirements of CNTs dispersion, pure suspension polymerization was, however, difficult. Therefore a combination of emulsion and suspension polymerization was tested. This included the same amount of surfactant and the same weight ratio of monomer to water which were used in emulsion polymerization.

2.2.2 Materials and methods

Multi-walled carbon nanotubes. Two types of multi-walled carbon nanotubes (MWCNTs) were used: thinner NC7000 (Nanocyl S.A. Belgium) with an average diameter of 9.5 nm and length of 1.5 μm according to the manufacturer, and thicker Bayer C 150 HP (Bayer, Germany) with an average diameter of 13–16 nm and length of 1 μm according to the manufacturer.

Other materials. Two monomers were tested: styrene with a similar structure as MWCNT, and methyl methacrylate. For dispersing MWCNTs and emulsion formation, two surfactants were used: sodium dodecyl benzene sulfate (DBSA) and sodium dodecyl sulfate (SDS). The buffer in polymerization reactions was sodium hydrogen carbonate. Two matrix polymers were milled before melt mixing: polystyrene (PS, Styron 678E, Dow Plastics) and poly(methyl methacrylate) (PMMA, IG840 LG Chemicals).

Ultrasound treatment to prepare the seed emulsion. Ultrasonic treatment was carried out with the probe of the ultrasonic horn (Hielscher UP400S) immersed directly into the mixed system. The power output was set at 100 W and the system was sonicated for 30 minutes. The seed emulsion contained MWCNTs, surfactant, buffer, and distilled water.

Emulsion polymerization. The initiator potassium peroxydisulfate (KPS) was dissolved in 10 mL water and the solution was fed into the reactor before the monomer feed. In order to achieve stable dispersion and polymerization, the reaction was carried out in a semi-batch way, i.e. the monomer was added dropwise with a membrane pump at 0.03 mL/min. Polymerizations were conducted under argon atmosphere for 18–19 hours at 60 °C with styrene and for 20–21 hours at 65 °C with methyl methacrylate.

Combined emulsion/suspension polymerization. The initiator azobisisobutyronitrile (AIBN) was dissolved in the monomer and the monomer solution was fed dropwise into the reactor. Polymerizations were conducted under argon atmosphere for 3 hours at 80 °C with styrene and for 20–21 hours at 75 °C with methyl methacrylate.

Post-treatment after polymerizations. After polymerization, depending on the characterization purposes or application, the emulsions were dried in an oven for at least 24 hours at 50 °C. To adjust the melt viscosity of the composite, glycerol was added to the emulsion before drying. The added amounts of glycerol were 30 or 50 wt.% of monomer, indicated as plast30 and plast50, respectively. The dried polymer powder was hot pressed at 165 °C for PMMA, and 170 °C for PS, to produce approximately 1 mm thick rectangular samples.

The use of masterbatches. Where composites were used as masterbatches, the final composites were prepared with a corotating twin-screw midi-

extruder. In the case of PS composites, different screw speeds (60/80/120 rpm) and mixing times (5/10/15 min) were tested at 190 °C. PMMA composites were mixed at 120 rpm for 10 min at 210 °C.

Characterizations. Molecular weights were determined by size exclusion chromatography (SEC). The particle size and rheology of the emulsions were analyzed with dynamic light scattering (DLS) and a rotation rheometer, respectively. A rotation rheometer was used to analyze the melt rheology of the final composites, which were produced by melt mixing from masterbatches. Mechanical properties were determined by dynamic mechanical analysis (DMA) or by tensile tests with Instron test machine. Electrical conductivity was determined by using a four-probe method. The measured conductivity was surface conductivity for dried emulsion samples and bulk conductivity for final composite samples, which were produced from masterbatches. The morphology of the composites was analyzed with SEM and TEM. A differential scanning calorimetry (DSC) was used to determine the glass transition temperatures of the masterbatches.

2.3 The effect of CNTs on the properties of the composites

2.3.1 Molecular weight and molecular weight distribution[†]

The molecular weight of a polymer is an essential character that affects other properties of the polymer. Thermal stability increases and mechanical properties improve with increasing molecular weight. However, there are hardly any studies on the molecular weight growth of a bulk polymer in the presence of CNTs in *in situ* polymerizations. Carbon black has been found to inhibit the polymerization of styrene without co-initiator or buffer in the emulsion polymerization of styrene. [107]

The effect of MWCNTs on molecular weight was observed by changing different variables, i.e. monomer, initiator, way of feeding the initiator, surfactant, and amount and type of MWCNTs in *in situ* polymerization (Tables 1-2). In general, the molecular weights increased as the MWCNT content in the polymerization reaction was increased. When present in the polymerization reaction, the MWCNTs stabilized the emulsions, and molecular weight distributions became narrower. Compatibility of the MWCNTs and the monomer had an effect on the polymerization and molecular weights, depending on the monomer used.

In the emulsion polymerization of styrene, MWCNTs stabilized the emulsion, and thinner nanotubes were more effective than thicker

nanotubes that had lower surface areas. Only 0.5 wt.% of the thinner NC7000 nanotubes had a major impact on the molecular weight of polystyrene (Table 1). The stabilization effect is based on the compatible structures of MWCNTs and styrene, in which individual nanotubes are covered by monomer clouds when the initiator arrives. There were no significant differences in molecular weights with different surfactants when thick MWCNTs were present in the polymerization reaction. However, when thinner nanotubes were used with SDS as surfactant, molecular weights were slightly lower and the molecular weight distributions were narrower, regardless of the amount of nanotubes.

In the emulsion polymerization of MMA, nanotubes did not affect the polymerization of MMA to the same extent, due to the incompatible structures of the monomer and the MWCNTs (Table 2). The addition of thin MWCNTs to the emulsion had only a minor effect on the molecular weight, and a significant amount of MWCNTs, over 6 wt.%, was needed before the effect was seen (Table 2).

In the combined emulsion/suspension polymerization of styrene, molecular weights were clearly lower than in emulsion polymerizations. One reason for the difference in molecular weights with different initiators was the difference in feeding. In emulsion polymerization, the initiator was fed before the monomer. In combined polymerization, the initiator was fed with the monomer and therefore there were probably more radical entries. Reactions between nanotubes and the initiator, AIBN, were the second reason. It has been observed that AIBN reacts with MWCNTs, [108,109] and covalently bonded polymer chains to CNTs were present. Therefore, there were probably fewer pure polystyrene chains in combined polymerizations to be determined with SEC, as the CNTs were filtered out before SEC analysis. There is probably a critical surface area of MWCNTs causing more initiator to be consumed in the reaction with nanotubes than in the polymerization of styrene. When there was 12 wt.% of the thinner NC7000 nanotubes in the combined polymerization of styrene, no polymer was observed. With 12 wt.% of the thicker Baytubes, the molecular weight dropped when SDS was used as surfactant.

Table 1. Molecular weights (M_w) and molecular weight distributions (PD) of the PS samples. The initiators were potassium persulfate (KPS) and azobisisobutyronitrile (AIBN), the surfactants were sodium dodecyl benzene sulfate (DBSA) and sodium dodecyl sulfate (SDS).¹

| Sample | Initiator | Surfactant | MWCNT type | MWCNT content (wt.%) | M_w (g/mol) | PD |
|-----------|-----------|------------|------------|----------------------|---------------|-----|
| S_KD0 | KPS | DBSA | Baytubes | - | 380 000 | 5.3 |
| S_KD3 | KPS | DBSA | Baytubes | 3 | 860 000 | 2.4 |
| S_KD6 | KPS | DBSA | Baytubes | 6 | 1 100 000 | 1.8 |
| S_KD12 | KPS | DBSA | Baytubes | 12 | 1 360 | 1.7 |
| S_AD0 | AIBN | DBSA | Baytubes | - | 220 000 | 4.4 |
| S_AD3 | AIBN | DBSA | Baytubes | 3 | 440 000 | 5.3 |
| S_AD6 | AIBN | DBSA | Baytubes | 6 | 650 000 | 5.8 |
| S_AD12 | AIBN | DBSA | Baytubes | 12 | 920 000 | 2.3 |
| S_KS0 | KPS | SDS | Baytubes | - | 580 000 | 2.4 |
| S_KS3 | KPS | SDS | Baytubes | 3 | 870 000 | 2.2 |
| S_KS6 | KPS | SDS | Baytubes | 6 | 1 080 | 2.0 |
| S_KS12 | KPS | SDS | Baytubes | 12 | 1 540 | 1.6 |
| S_AS0 | AIBN | SDS | Baytubes | - | 350 000 | 2.5 |
| S_AS3 | AIBN | SDS | Baytubes | 3 | 770 000 | 2.3 |
| S_AS6 | AIBN | SDS | Baytubes | 6 | 920 000 | 2.0 |
| S_AS12 | AIBN | SDS | Baytubes | 12 | 460 000 | 3.3 |
| S_KDnc0 | KPS | DBSA | NC7000 | - | 380 000 | 5.3 |
| S_KDnc1.5 | KPS | DBSA | NC7000 | 1.5 | 1 270 | 3.1 |
| S_KDnc3 | KPS | DBSA | NC7000 | 3 | 1 510 000 | 4.4 |
| S_KDnc6 | KPS | DBSA | NC7000 | 6 | 146 000 | 1.8 |
| S_ADnc0 | AIBN | DBSA | NC7000 | - | 220 000 | 4.4 |
| S_ADnc1.5 | AIBN | DBSA | NC7000 | 1.5 | 630 000 | 4.8 |
| S_ADnc3 | AIBN | DBSA | NC7000 | 3 | 570 000 | 3.7 |
| S_ADnc6 | AIBN | DBSA | NC7000 | 6 | 270 000 | 3.9 |
| S_KSnc0 | KPS | SDS | NC7000 | - | 580 000 | 2.4 |
| S_KSnc0.5 | KPS | SDS | NC7000 | 0.5 | 1 160 000 | 2.0 |
| S_KSnc1.5 | KPS | SDS | NC7000 | 1.5 | 1 200 | 1.8 |
| S_KSnc3 | KPS | SDS | NC7000 | 3 | 1 240 | 2.0 |
| S_KSnc6 | KPS | SDS | NC7000 | 6 | 1 750 000 | 1.3 |
| S_ASnc0 | AIBN | SDS | NC7000 | - | 350 000 | 2.5 |
| S_ASnc0.5 | AIBN | SDS | NC7000 | 0.5 | 540 000 | 3.5 |
| S_ASnc1.5 | AIBN | SDS | NC7000 | 1.5 | 690 000 | 7.2 |
| S_ASnc3 | AIBN | SDS | NC7000 | 3 | 620 000 | 3.0 |
| S_ASnc6 | AIBN | SDS | NC7000 | 6 | 650 000 | 5.3 |

Table 2. Molecular weights (M_w) and molecular weight distributions (PD) of the PMMA samples. The initiators were potassium peroxydisulfate (KPS) and azobisisobutyronitrile (AIBN), the surfactants were sodium dodecyl benzene sulfate (DBSA) and sodium dodecyl sulfate (SDS).¹

| Sample | Initiator | Surfactant | MWCNT type | MWCNT content (wt.%) | M_w (g/mol) | PD |
|-----------|-----------|------------|------------|----------------------|---------------|-----|
| M_KD0 | KPS | DBSA | Baytubes | - | 144 000 | 3.7 |
| M_KD3 | KPS | DBSA | Baytubes | 3 | 152 000 | 2.8 |
| M_KD6 | KPS | DBSA | Baytubes | 6 | 504 000 | 2.8 |
| M_KD15 | KPS | DBSA | Baytubes | 15 | 661 000 | 2.9 |
| M_KS0 | KPS | SDS | Baytubes | - | 263 000 | 2.4 |
| M_KS3 | KPS | SDS | Baytubes | 3 | 397 000 | 2.7 |
| M_KS6 | KPS | SDS | Baytubes | 6 | 469 000 | 3.8 |
| M_KS15 | KPS | SDS | Baytubes | 15 | 1 438 000 | 2.5 |
| M_AS0 | AIBN | SDS | Baytubes | - | 235 000 | 2.3 |
| M_AS3 | AIBN | SDS | Baytubes | 3 | 455 000 | 2.7 |
| M_AS6 | AIBN | SDS | Baytubes | 6 | 487 000 | 2.8 |
| M_AS15 | AIBN | SDS | Baytubes | 15 | 493 000 | 2.9 |
| M_KDnc0 | KPS | DBSA | NC7000 | - | 144 000 | 3.7 |
| M_KDnc1.5 | KPS | DBSA | NC7000 | 1.5 | 155 000 | 2.2 |
| M_KDnc3 | KPS | DBSA | NC7000 | 3 | 145 000 | 2.8 |
| M_KDnc4.5 | KPS | DBSA | NC7000 | 4.5 | 159 000 | 2.7 |
| M_KDnc6 | KPS | DBSA | NC7000 | 6 | 160 000 | 3.6 |
| M_KDnc10 | KPS | DBSA | NC7000 | 10 | 217 000 | 3.7 |
| M_KSnc0 | KPS | SDS | NC7000 | - | 263 000 | 2.4 |
| M_KSnc3 | KPS | SDS | NC7000 | 3 | 373 000 | 3.1 |
| M_KSnc6 | KPS | SDS | NC7000 | 6 | 597 000 | 3.6 |
| M_ADnc0 | AIBN | DBSA | NC7000 | - | 235 000 | 2.3 |
| M_ADnc1.5 | AIBN | DBSA | NC7000 | 1.5 | 412 000 | 2.4 |
| M_ADnc3 | AIBN | DBSA | NC7000 | 3 | 486 000 | 2.3 |
| M_ADnc4.5 | AIBN | DBSA | NC7000 | 4.5 | 461 000 | 2.2 |
| M_ADnc6 | AIBN | DBSA | NC7000 | 6 | 395 000 | 2.5 |
| M_ADnc10 | AIBN | DBSA | NC7000 | 10 | 500 000 | 2.4 |

In the combined polymerization of MMA, the initiator AIBN reacted with the nanotubes, the nanotubes acted as a carrier for the initiator, and the molecular weight increased as the amount of MWCNTs increased, with the molecular weight distribution remaining constant. When thicker nanotubes were used, the effect of nanotubes was even smaller. The molecular weights increased with increasing amount of nanotubes, but the difference between the initiators was not as pronounced as for thin nanotubes.

The role of surfactant. The surfactant did not cause the increase in molecular weight even though there is a need to consume more surfactant

to disperse the increased amount of MWCNTs and less surfactant is left to form polymer particles in the emulsion. However, the amount of surfactant was high compared with the amounts of MWCNTs and monomers, and the difference in consumption had only a minor effect on the molecular weight. Otherwise there should be higher molecular weights when using thinner MWCNTs in the polymerization reaction, as they need more surfactant for dispersion. It seems that DBSA was a better dispersant for the nanotubes by yielding more stable molecular weight distributions and, at the same time, covering the surface of the nanotubes so that fewer nanotubes participated in the polymerization reaction. Due to π -stacking the benzene rings of DBSA covered the surface of the nanotubes better, decreasing the reactions between the initiator and MWCNTs and preventing a drop in molecular weight for 12 wt.% Baytubes with DBSA.

2.3.2 Emulsion properties[†]

Emulsion structure. DLS was used to analyze changes in particle size during the monomer feed and the polymerization of styrene and methyl methacrylate. It can be seen from the DLS data that without MWCNTs in the seed emulsions small, 2-nm diameter surfactant micelles were formed. Pure surfactant micelles did not form in the initial seed emulsions with MWCNTs, as the surfactant accumulates around MWCNTs. Polymerization started already during monomer feed, whereby the emulsion contained mostly growing polymer particles without large monomer droplets. The particle size distribution did not change significantly after 3 ml of monomer feed. During polymerization, after monomer feed, the particle size distribution remained constant (Fig. 6).

The diameter of polystyrene particles was 20 – 40 nm and the number of pure polystyrene particles decreased as the amount of MWCNTs increased (Fig. 7). When the amount of thicker MWCNTs increased in the emulsion, particles having a diameter of 500 nm formed. When AIBN was used as initiator, there were slightly more distinct sets of 500-nm particles. However, when thinner MWCNTs were used, only polymer particles with a diameter under 100 nm were observed. This is due to the fact that DLS does not reliably measure particle sizes over 10 μm . As thinner MWCNTs have more surface area to adsorb styrene, the size of the aggregated particles, including polystyrene particles and nanotubes, may exceed the measuring range. There is the set of larger particles of 5 μm diameter that can be assigned to the aggregates of MWCNTs and polymer particles attached to MWCNTs.

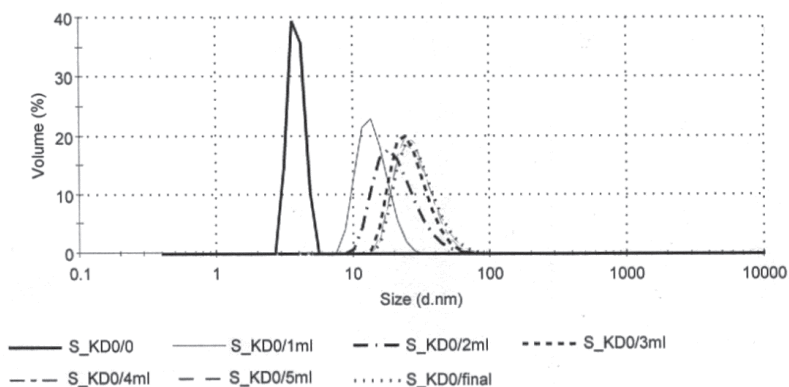


Figure 6. The change in particle size distribution during styrene feed and after total polymerization time. Emulsion polymerization with KPS as initiator, sodium dodecyl benzene sulfate (DBSA) as surfactant, and without MWCNTs.¹

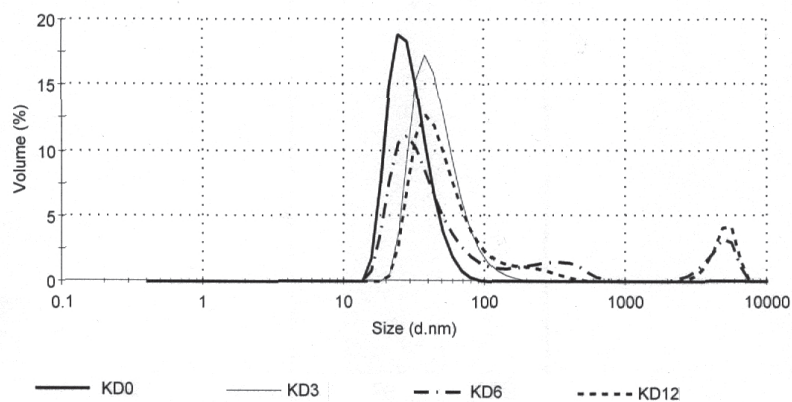


Figure 7. Particle size distribution after polymerizations of PS emulsion samples with 0, 3, 6, and 12 wt.% MWCNTs (Baytubes) denoted KDo, KD3, KD6, and KD12, respectively. Emulsion polymerization with KPS as initiator and sodium dodecyl benzene sulfate (DBSA) as surfactant. (Unpublished figure).

When MMA was used as a monomer, the formed PMMA particles were slightly smaller than PS particles. In general, the particle size distribution of PMMA was similar to that obtained with PS, but the particle size changed differently during the monomer feed and as the amount of MWCNTs increased. The larger particles, 5 μm in diameter, were more predominant when AIBN was used as initiator. When KPS was used as initiator and DBSA as surfactant, the particle size distribution was independent of the amount of MWCNTs, and thinner MWCNTs exhibited more distinct sets of particles. The characterization of molecular weights yielded similar results, i.e. molecular weight was not dependent on the amount of thinner MWCNTs.

The amount of surfactant was not the main reason for the increase in the molecular weight analyzed with SEC. The DLS results are in agreement with the SEC results. Thinner MWCNTs consume more surfactant during dispersion, but the amount of surfactant was so high that it only partially affected the size of particles, i.e. there was less surfactant and the size of polymer particles would grow for this reason. Otherwise, the increase of MWCNTs in the polymerization reactions would increase the particle size more strongly and decrease the amount of smaller particles.

Emulsion rheology. Due to dilute solutions, the viscosity of the emulsions was low. At lower shear rates, the MWCNTs increased the viscosity as the particle sizes and molecular weights increased. At higher shear rates, the viscosity was fairly similar for all emulsions regardless of the amount of MWCNTs.

Viscosity of the PMMA emulsion increased with increasing amount of MWCNTs. On the other hand, the distribution of particle sizes in the emulsions did not change, as indicated by the similar shape of curves with different MWCNT contents (Fig. 8). The rheology results of the PMMA emulsions supported the conclusions that thinner MWCNTs were not affected in the polymerization reaction. A similar result was seen in the DLS data.

Viscosity of the PS emulsions increased with increasing amount of MWCNTs, but not to the same extent as with the PMMA emulsions. The shape of the viscosity curves changed, as the amount of MWCNTs changed. The particle size distribution becomes narrower, as the slope of the curve becomes sharper and shifts to a higher shear rate. This occurred with the viscosity curve of the PS emulsions, as the amount of MWCNTs increased. The rheology results of the PS emulsions confirm the stabilizing effect of MWCNTs, which causes the increase in the molecular weight of PS.

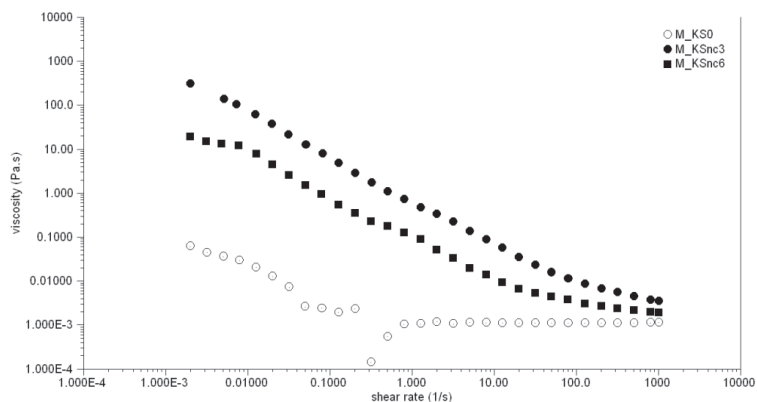


Figure 8. Viscosity of the PMMA emulsions with 0, 3, and 6 wt.% MWCNTs (NC7000), denoted M_KS0, M_KSnc3, and M_KSnc6, respectively. Emulsion polymerization with KPS as initiator and sodium dodecyl sulfate (SDS) as surfactant.¹

2.3.3 Composite properties^{1,II}

Morphology. SEM images from the dried emulsions revealed a pearl-like structure (Fig. 9). The size of the polymer pearls is in the same range as that observed from the emulsion with DLS. The polymer pearls are to some extent bonded to dispersed MWCNTs, and they efficiently prevent the agglomeration of MWCNTs. TEM images from the composites (Fig. 10), which had been melt processed after drying the emulsions, confirmed that *in situ* emulsion polymerization provides stable dispersion of the high concentrations of MWCNTs after mild ultrasound treatment.

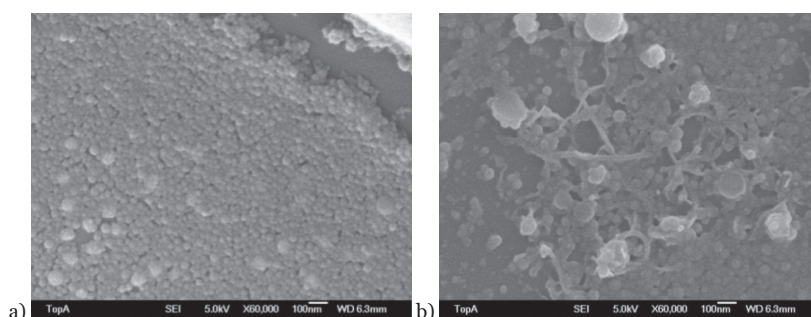


Figure 9. SEM images of dried PS emulsions; combined polymerization with AIBN as initiator, dodecyl benzene sulfate as surfactant, and a) without MWCNTs, b) with 3 wt.% of MWCNTs (Baytubes).¹

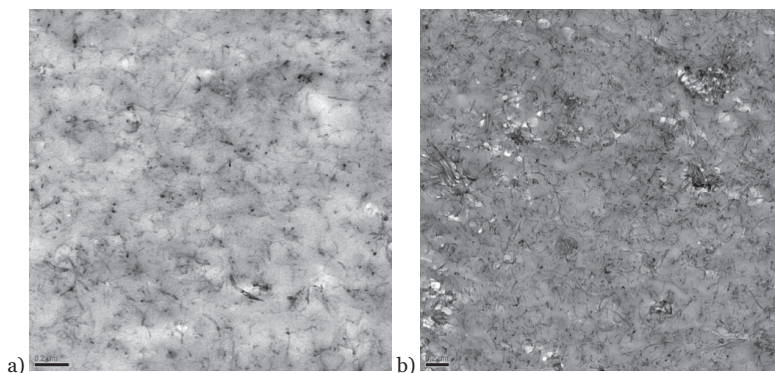


Figure 10. TEM images of PMMA/MWCNT composites, emulsion polymerization with KPS as initiator, dodecyl benzene sulfate as surfactant, and a) 10 wt.% of MWCNTs (NC7000), b) 15 wt.% of MWCNTs (Baytubes).¹

Electrical conductivity of CNT/polymer composites. For PS composites (Fig. 11) with thinner CNTs, the percolation threshold was between 0.5 and 1.5 wt.% MWCNTs when SDS was used as surfactant. The percolation threshold shifted to 1.5–3 wt.% MWCNTs when DBSA was used as surfactant. The molecular weight had an insignificant effect on conductivity compared with the surfactant, but it seems that with a similar structure of PS and CNT, a lower molecular weight PS can cover and disperse CNTs better, and therefore resistances were higher in composites polymerized using a combined polymerization technique. With thicker CNTs, the percolation threshold was significantly higher. The percolation threshold was between 3 and 6 wt.% MWCNTs, and the overall resistances were higher with thicker tubes. The effect of different parameters was more pronounced and there is more deviation in resistances. With thicker tubes, lower molecular weight decreased the resistance of the composite, as did the use of SDS as surfactant.

For PMMA composites (Fig. 12), the polymerization method significantly affected the electrical conductivity. The use of the combined polymerization technique resulted in better electrical conductivities for the composites. With the dissimilar structure of PMMA and CNTs, the PMMA composites had higher percolation thresholds than the PS composites. For PMMA composites with thinner CNTs the percolation threshold was between 1.5 and 3 wt.% MWCNTs, and with thicker tubes, the percolation threshold shifted to 3–6 wt.% MWCNTs.

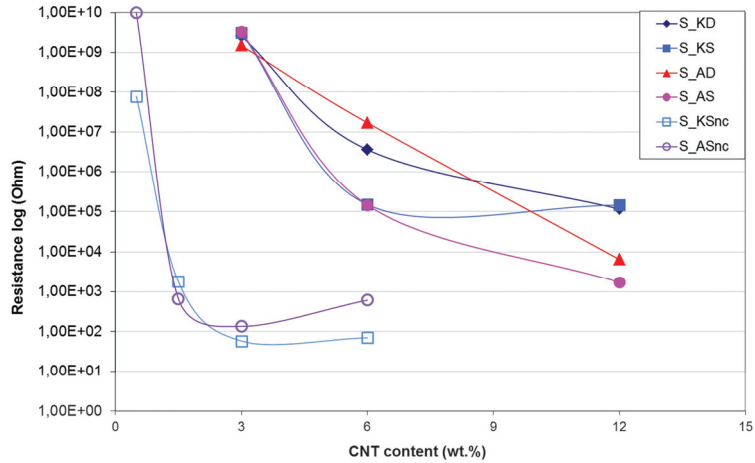


Figure 11. Electrical conductivities of MWCNT/PS composites. The samples were denoted K and A, based on emulsion polymerization with KPS as initiator and combined emulsion/suspension polymerization with AIBN as initiator, respectively; D and S denote the used surfactant, sodium dodecyl benzene sulfate and sodium dodecyl sulfate, respectively; no label and nc denote MWCNTs, Baytubes and NC7000, respectively.¹¹

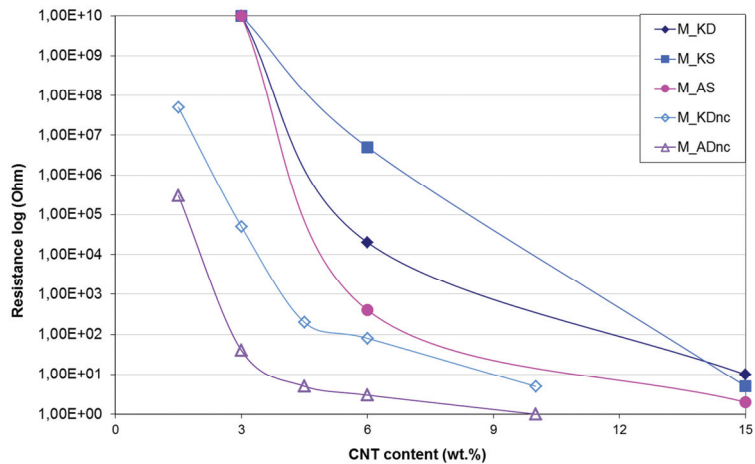


Figure 12. Electrical conductivities of MWCNT/PMMA composites. The samples were denoted K and A, based on emulsion polymerization with KPS as initiator and combined emulsion/suspension polymerization with AIBN as initiator, respectively; D and S denote the used surfactant, sodium dodecyl benzene sulfate and sodium dodecyl sulfate, respectively; no label and nc denote MWCNTs, Baytubes and NC7000, respectively.¹¹

Mechanical properties of CNT/polymer composites. There are several factors that affect the mechanical properties, such as stiffness and strength, of the composite. Macroscopic fillers are used as reinforcement to increase stiffness, but usually the material becomes more brittle. The poor dispersion of fillers can decrease both strength and stiffness, which is more pronounced in the case of nanofillers. Therefore, the real dispersion at the nano level is essential for nanoparticles to have the reinforcement effect.

The adhesion between the components is the critical factor for improving the mechanical properties. The mechanical properties can be varied by changing the crystallinity of the polymer matrix, which can have a significant effect on mechanical properties and electrical conductivities, [33,110-112] but the molecular weight has an effect as well.

As the molecular weights and polydispersities of the composites varied significantly with different MWCNTs, MWCNT loading, and initiators, it was difficult to estimate to what degree the improvement in mechanical properties was induced by MWCNTs. Even the surfactants can affect the mechanical properties by plasticizing the polymer.

The molecular weights increased as the amount of CNT increased, and mechanical properties, measured with DMA, were improved. By adding a low amount of thin MWCNTs to the polystyrene, Young's modulus was improved and the strain at break values doubled (Fig. 13). In emulsion polymerization, the molecular weights increased significantly, which was partially responsible for the increased modulus values. Molecular weights increased only moderately in combined polymerizations when AIBN was used as initiator. However, AIBN can form covalent bonds with CNTs and there are more polystyrene chains attached covalently to CNTs, and the adhesion between the polystyrene matrix and CNTs was enhanced. Therefore, the combined polymerization method resulted in the best combination of mechanical properties.

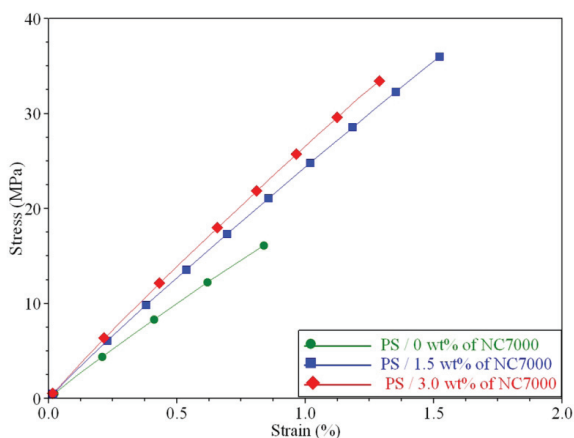


Figure 13. Stress-strain curves of MWCNT/PS composite samples, combined polymerizations with AIBN as initiator and with 0, 1.5, and 3 wt.% of thinner NC7000 tubes.¹¹

For PMMA composites, the combined polymerization method was even more efficient than for polystyrene in terms of improving Young's modulus. Molecular weights were higher with the use of the combined polymerization technique, which increased Young's modulus. However, improved adhesion decreased the strain values of the PMMA composites.

2.4 The use of CNT composite as a masterbatch^{III}

Due to the ability to tailor the electrical and mechanical properties of MWCNT composites, combined with the reasonably stable dispersion of MWCNTs, these composites were used as masterbatches in order to increase the amount of conductive composite (Table 3). In the case of PS masterbatches, two different molecular weight masterbatches were tested with different amounts of MWCNTs. In both cases of PS and PMMA masterbatches, the viscosity was modified by adding glycerol.

Table 3. Molecular weights (M_w) analyzed with SEC and glass transition temperatures (T_g) analyzed with DSC of the matrix polymers and the masterbatches (MB).^{III}

| Sample | MWCNT content (wt.%) | M_w (g/mol) | T_g (°C) |
|--|----------------------|---------------|------------|
| PS, matrix | - | 260 000 | 87 |
| MB _{PS} (emulsion polymerized) | 12 | 1,450 000 | 89 |
| MB _{PS} (combined emulsion/suspension polymerized) | 6 | 630 000 | 107 |
| MB _{PS} (combined emulsion/suspension polymerized), plasticized | 6 | 630 000 | 106 |
| PMMA, matrix | - | 160 000 | 106 |
| MB _{PMMA} (emulsion polymerized) | 10 | 280 000 | 123 |
| MB _{PMMA} (emulsion polymerized), plasticized | 10 | 280 000 | 118 |

Conductivity of the final MWCNT composites. When possibilities are only limited to affect shear forces to disperse the MWCNTs into the polymer matrix in melt mixing, the compatible structure between components is one factor to be considered. In the directly melt mixed MWCNT composites, the MWCNTs formed agglomerates and acted more like macroscopic particles than individual nanoparticles though the resistance decreased as MWCNT content increased. Due to the compatible structure of the MWCNTs and polystyrene, MWCNTs disperse more easily in the polystyrene than in

PMMA, and the directly melt mixed PS-MWCNT composites were conductive with a MWCNT loading of 1–2 wt.% (Table 4). π -stacking between MWCNTs and PS limits the reagglomeration of CNTs. In the case of MWCNTs with PMMA, which have dissimilar structures, the directly melt mixed PMMA-MWCNT composites were not conductive even at 4 wt.% CNTs (Table 5).

The matrix polymers have quite low molecular weights compared with the masterbatches. The increase in molecular weight increased the viscosity of the polymer melt, and with the insufficient viscosity ratio of the components, the masterbatch formed a dispersed phase. The directly melt mixed PS-MWCNT composites were conductive below 2 wt.% MWCNTs, and the high molecular weight PS-masterbatch composite was conductive below 3 wt.% MWCNTs. When the molecular weight of the PS-masterbatch was lower, the conductivity was achieved below 2 wt.% MWCNTs. The MWCNTs remained mostly in the PS-masterbatch phase due to the *in situ* polymerization method of the masterbatch. The initiator formed additional bonding with the MWCNTs, whereby some polymer chains were covalently attached to the MWCNTs, preventing the MWCNTs from migrating to the matrix polymer.

Table 4. Resistivity of polystyrene samples; melt mixing parameters were 10 min and 120 rpm, if not marked otherwise. MWCNTs were introduced directly (PS) or by using masterbatches (PS/MB_{PS}).^{III}

| Sample | MWCNT content (wt.%) | Resistivity (Ω cm) |
|--|----------------------|----------------------------|
| 1 PS | 1 | $> 10^9$ |
| 1 PS/MB _{PS} | 1 | $> 10^9$ |
| 2 PS | 2 | $1.1 \cdot 10^5$ |
| 2 PS/MB _{PS} | 2 | $2.0 \cdot 10^7$ |
| 2 PS/MB _{PS} 5min/120rpm | 2 | $> 10^9$ |
| 2 PS/MB _{PS} 5min/60rpm | 2 | $> 10^9$ |
| 2 PS/MB _{PS} 10min/60rpm | 2 | $> 10^9$ |
| 2 PS/MB _{PS,AIBN} * | 2 | $2.6 \cdot 10^7$ |
| 2 PS/MB _{PS,AIBN,plasticized} * | 2 | $1.1 \cdot 10^5$ |
| 3 PS | 3 | 650 |
| 4 PS | 4 | 180 |

*) Masterbatches were *in situ* polymerized by using combined emulsion/suspension polymerization method.

The use of the PMMA-masterbatch gave clearly lower resistance values than the use of the directly melt mixed MWCNTs. The conductive composite was

achieved below 4 wt.% MWCNTs when using a PMMA-masterbatch. By lowering the viscosity of the PMMA-masterbatch with glycerol, the conductive composite was achieved below 3 wt.% MWCNTs. A moderately low resistance was achieved even with 2 wt.% MWCNTs, when a higher amount of glycerol was added to the PMMA-masterbatch.

Table 5. The resistivity of PMMA samples. MWCNTs were introduced directly (PMMA) or by using masterbatches (PS/MB_{PMMA}).^{III}

| Sample | MWCNT content (wt.%) | Resistivity (Ωcm) |
|--|----------------------|-----------------------------------|
| 1 PMMA | 1 | $> 10^9$ |
| 1 PMMA/MB _{PMMA} | 1 | $> 10^9$ |
| 2 PMMA | 2 | $> 10^9$ |
| 2 PMMA/MB _{PMMA} | 2 | $> 10^9$ |
| 2 PMMA/MB _{PMMA} ,plasticized (30 wt.%) | 2 | $1.1 \cdot 10^8$ |
| 2 PMMA/MB _{PMMA} ,plasticized (50 wt.%) | 2 | $4.1 \cdot 10^7$ |
| 3 PMMA | 3 | $> 10^9$ |
| 3 PMMA/MB _{PMMA} | 3 | $> 10^9$ |
| 3 PMMA/MB _{PMMA} ,plasticized (30 wt.%) | 3 | 320 |
| 4 PMMA | 4 | $> 10^9$ |
| 4 PMMA/MB _{PMMA} | 4 | $1.3 \cdot 10^5$ |

Rheology of MWCNT masterbatches. As the resistance decreased by adding glycerol to the masterbatch, a better viscosity ratio of the components was achieved. Due to the limitations of the instrument, only the viscosities of the final composites were measured. Indirect measurements of the rheological properties of the masterbatches revealed that the addition of MWCNTs increased the viscosity of the composites compared with the matrix polymers. The viscosity of the final composite was highest with the masterbatches, as the higher molecular weight of the polymer induces higher viscosity. PMMA composites behaved in a very straightforward manner (Fig. 14). The addition of MWCNTs increased the viscosity, and the viscosity was highest with the PMMA-masterbatch. The PMMA-masterbatch has a higher molecular weight than matrix PMMA and most of the MWCNTs are located in the PMMA-masterbatch phase. Both of these factors lead to an increase in viscosity. However, addition of glycerol to the PMMA-masterbatch resulted in a lower viscosity than that of the directly melt mixed MWCNT composite with the same amount of MWCNTs. The glass transition temperatures, which were measured directly from the masterbatches and the matrix polymers, follow the molecular weight and

plasticization (Table 3). Matrix PMMA has the lowest T_g , whereas the PMMA-masterbatch, having a higher molecular weight and the MWCNTs, has the highest T_g . The use of plasticized masterbatch resulted in a lower T_g .

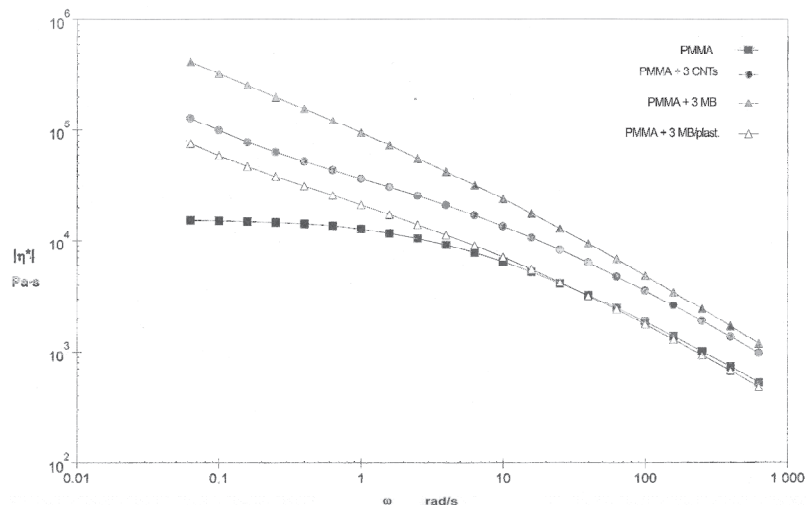


Figure 14. Viscosities of PMMA matrix and final PMMA composites with 3 wt.% MWCNTs: Directly melt mixed MWCNTs (PMMA + 3 CNTs), using masterbatch (PMMA + 3 MB), and using plasticized masterbatch (PMMA + 3 MBplast).¹¹¹

Polystyrene, due to its interactions with MWCNTs, behaved differently from PMMA. Addition of MWCNTs increased the viscosity of matrix polystyrene. There was also a slight difference between the high molecular weight PS-masterbatch and the lower molecular weight PS-masterbatch. However, addition of glycerol to the lower molecular weight PS-masterbatch increased the viscosity of the final composite. It is possible that the finer morphology of the masterbatch in the final composite was achieved with the help of glycerol, whereby the dispersion of MWCNTs in the final composite was improved, thus increasing the viscosity of the final composite.

Mechanical properties of the final composites. The compounding of pure MWCNTs with a matrix polymer seemed to slightly weaken the mechanical properties. In the case of PMMA, tensile modulus was mainly affected by the plasticizer and not by MWCNTs (Fig. 15). On the other hand, the tensile strength of PMMA composites decreased with the addition of MWCNTs, and the decrease was more pronounced with the use of a PMMA-masterbatch than with directly melt mixed MWCNTs. However, the amount of masterbatch in the final composite increased with higher amounts of MWCNTs. Therefore, part of the changes in mechanical properties comes

from the properties of the masterbatch and not only from the MWCNTs. Tensile strength of the composite was better, if there was added plasticizer in the PMMA-masterbatch. The same behavior can be observed for tensile strain at break.

In the case of polystyrene, the tensile modulus was affected more by the high molecular weight PS-masterbatch than by MWCNTs (Fig. 16), with the tensile modulus being slightly higher, if the high molecular weight PS-masterbatch was used. The addition of pure MWCNTs to matrix PS did not affect the tensile modulus, nor did the use of the lower molecular weight PS-masterbatch. The improvement of mechanical properties depending on the molecular weight of the PS-masterbatch was seen more clearly for tensile strength. Tensile strength decreased by adding pure MWCNTs to matrix PS, which implied that MWCNTs were agglomerated and not dispersed as individual tubes. When the amount of MWCNTs increased to 4 wt.%, they started again to strengthen the composite as micro-size filler. The addition of the plasticizer to the lower molecular weight PS-masterbatch decreased the mechanical properties of the final composite.

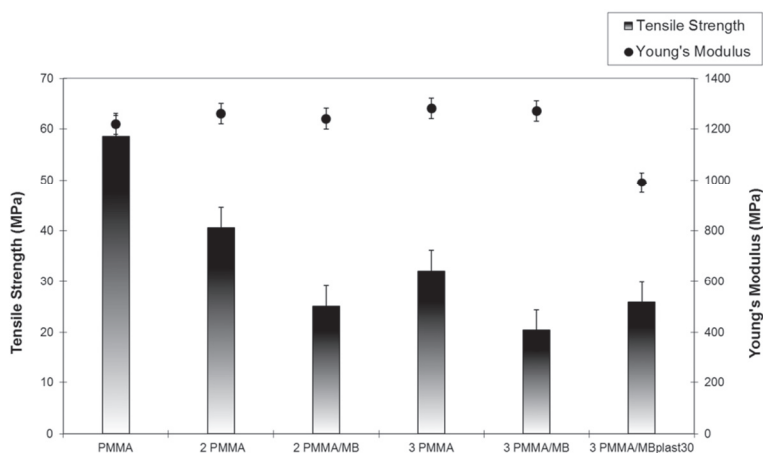


Figure 15. Mechanical properties of PMMA matrix and final PMMA composites with 2 and 3 wt.% MWCNTs: Directly melt mixed MWCNTs (PMMA), using masterbatch (PMMA/MB), and using plasticized masterbatch (PMMA/MBplast30).^{III}

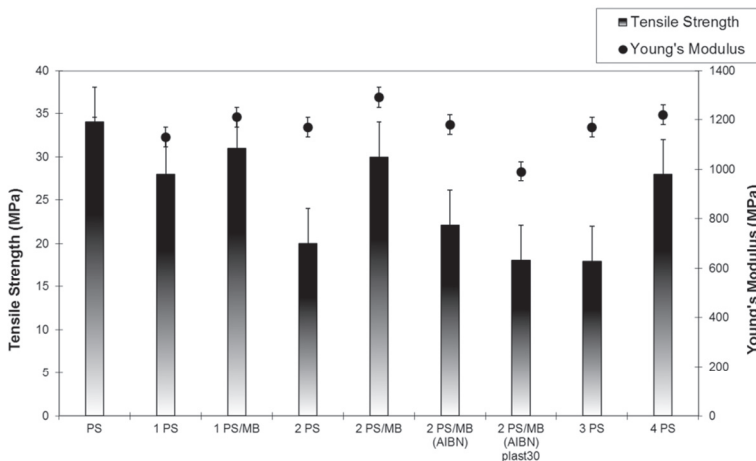


Figure 16. Mechanical properties of PS matrix and final PS composites with 1-4 wt.% MWCNTs: Directly melt mixed MWCNTs (PS), using emulsion polymerized masterbatch (PS/MB), and using combined emulsion/suspension polymerized and plasticized masterbatch (PS/MB(AIBN), PS/MB(AIBN)plast30).¹¹¹

The use of a masterbatch for the production of a conductive MWCNT composite was beneficial in the case of PMMA. For the plasticized masterbatch, excellent conductivity was attained with 3 wt.% of MWCNTs. If the same amount of MWCNTs was melt mixed directly with the matrix PMMA, the composite was an insulator. The use of the plasticizer in the masterbatch decreased Young's modulus of the conductive composite with 3 wt.% MWCNTs, but tensile strength and strain at break were at the same level compared with non-conductive composite with 3 wt.% directly melt mixed MWCNTs. The use of masterbatch was not so beneficial in the case of PS. The proper conductivity level was obtained with 2 wt.% MWCNTs by using both mixing methods, the masterbatch, or directly mixed MWCNTs. Also the plasticized PS-masterbatch decreased Young's modulus in the final composite, but did not affect tensile strength or strain compared with composites with directly melt mixed MWCNTs.

3. Polyaniline blends produced by melt mixing^{IV}

3.1 The achievements in blending polyaniline with other polymers

Intrinsically conductive polymers and their blends can be used when electrical conductivity is sought without added particles. Polyaniline (PANI) is one of the most useful intrinsically conductive polymers due to its stability and ease of polymerization in comparison with other intrinsically conductive polymers. Protonic acids, such as dodecyl benzene sulfonic acid (DBSA) and camphorsulfonic acid (CSA), are often used to dope PANI. The PANI/CSA complex has a very good conductivity, above 100 S/cm, and therefore it is often used in solution processes. [69,113] On the other hand, an excess of DBSA in doping can be as effective, as it makes the PANI complex melt processable to some extent. [63,114] But even though the dopant is able to plasticize PANI, the PANI complex remains very brittle. Therefore, PANI is blended with other polymers to give mechanical strength.

In electrically conductive PANI blends, the morphology is even more important than in composites based on the MWCNT masterbatch. The PANI phase must be continuous for the blend to be conductive, but the matrix phase also needs to be continuous for improved mechanical properties. Since adhesion is essential for achieving good mechanical properties of polymer blends, compatibilization is a necessary part of blending. [115]

In the case of the PANI complex, the interactions that are needed for increasing adhesion between blend components can decrease the conductivity of the PANI complex or even destroy it when dopant is reacting with the matrix or compatibilizer. Maleic anhydride (MAH), which is often used for compatibilization, forms covalent bonds with the PANI backbone in the PANI/DBSA complex. [116] However, when MAH has an effect on the rheology or crystallization of a matrix polymer, it can maintain the conductivity of the PANI complex. [117] Even hydrogen bonds may have a negative effect on the delocalization of electrons in the PANI chain. [118]

Therefore, polar polymer matrices are used in PANI blends since the PANI complex itself is polar. [119,120]

There are only a few studies on the mechanical properties of PANI blends with nonpolar polymers such as polyolefins like polyethylene and polypropylene due to the lack of adhesion between the PANI phase and polyolefin matrix in melt processing. Mostly the studies concentrate on enhancing the conductivity of the blend, which is done by using dopants that have long alkyl chains. [65] With a nonpolar polymer matrix, PANI is usually doped with DBSA or toluenesulfonic acid (TSA).

Most of the studies on compatibilization of PANI blends have focused on maintaining the conductivity at a reasonable level, ignoring mechanical properties. By using copolyamide 6/6.9 as compatibilizer in blends of PANI/TSA and LDPE, the highest conductivity (c. 10^{-4} S/cm) was obtained in a blend containing 20 wt.% of PANI/TSA and LDPE/copolyamide ratio of 75/25, but no mechanical properties of the blends were reported. [121] By using ethylene/vinyl acetate copolymer (EVA) as compatibilizer in the blends of PANI/TSA and LDPE, excellent conductivities of the blends were obtained, reaching up to 10^{-1} S/cm. However, the mechanical properties of the compatibilized blends were worse than those in pure LDPE. Tensile strength was reduced by c. 26 % and elongation by 66 % at a PANI content of 15 wt.%. [121,122]

EVA was used to compatibilize blends of PANI/DBSA and LDPE as well. In blends of 15 wt.% PANI and 10 wt.% EVA, the conductivity was c. 10^{-6} S/cm. The addition of EVA slightly affected the yield elongation, but the mechanical properties of the blends were worse than in pure LDPE. [123]

Metallocene polymerization can offer a unique material for improving adhesion in PANI/PE blends. With metallocene catalysts it is possible to prepare polyethylene containing hydroxyl or carboxylic acid groups and exhibiting a controlled molecular weight. Therefore, the compatibilizer itself can improve the mechanical properties of a blend. Metallocene catalysts are used in coordination polymerization, i.e. stereospecific polymerization. In coordination polymerization, the initiator is called a catalyst due to the importance of the initiator. Metallocene catalysts consist of transition metal complexes with two ligands that are η^5 -cyclopentadienyls or substituted cyclopentadienyls. Based on the structure of the catalyst, the monomer is attached to the growing polymer chain in the exact stereoselectively defined orientation. Metallocene catalyst

combined with methylaluminoxane (MAO) has high catalytic activity and stability. With the cocatalytic system it is possible to prepare polymers with a narrow molecular weight distribution, stereospecific polymers and copolymers that contain functionalized, even polar comonomers. [105,124]

In an attempt to enhance adhesion in PANI/PE blends, the use of functional polyethylenes polymerized with metallocene catalysts as compatibilizers was studied. Functionalized metallocene polyethylenes contain only ~0.20 mol-% functionality and the amount of hydrogen bonds with the PANI complex is so low that the effect on the delocalization of electrons in the PANI chains is minimal. However, a minimal amount of functionalities in polyolefins changes the polarity of the polyolefin. [125,126] On the other hand, there should be proper functional groups in the PANI complex for increasing adhesion. The third criterion for forming a better PANI/PE blend by melt mixing is the plasticized PANI complex, otherwise the PANI can be counted as an infusible particle in the polymer matrix. As the PANI/CSA complex has good conductivity, the aim was to produce a plasticized PANI/CSA complex and prepare by melt mixing a conductive PANI/PE blend having good mechanical properties (Fig. 17). Therefore, the PANI content in blends was made high enough for the blends to be conductive, and the research was focused on the compatibilization properties of functionalized metallocene polyolefins.

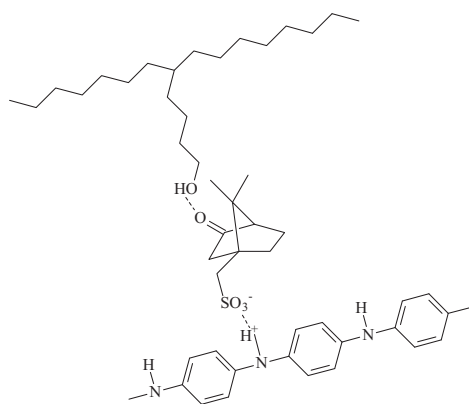


Figure 17. Compatibilization of the PANI/CSA complex and OH-functionalized polyethylene.^{IV}

3.2 Materials and processing

Polyethylenes. The polyethylenes used as matrix components, LDPE and metallocene polyethylene, HDPE, and the maleic anhydride functionalized polyethylene PE-g-MAH used as compatibilizer, were supplied by Borealis Polymers Oy. The functionalities in the prepared metallocene polyethylenes were hydroxyl groups (OH; M_w 144 000 g/mol, 0.2 mol-%) and carboxylic acid groups (COOH; M_w 117 000 g/mol, 0.2 mol-%).

PANI complexes. Plasticized polyanilines doped with *p*-toluenesulfonic acid (p-TSA) and phenolsulfonic acid (PSA), and different unplasticized polyanilines doped with camphorsulfonic acid (CSA), designated PANI/CSA1 and PANI/CSA2, in powder form, were supplied by Panipol Oy. Unplasticized polyanilines were plasticized in cooperation with Panipol Oy following their industrial process. The plasticization of PANI/CSA complexes was carried out in a melt mixer with ZnO₂ and DBSA as plasticizing agents. PANI/TSA, PANI/PSA, and PANI/CSA complexes were prepared in the laboratory scale by Panipol Oy, and plasticization of the complexes was more important than high conductivity (Fig. 18).

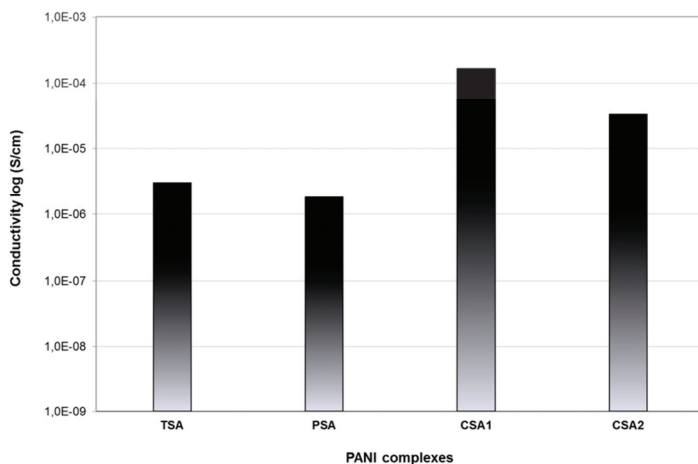


Figure 18. The conductivities of pure PANI complexes with toluenesulfonic acid (TSA), phenolsulfonic acid (PSA), and camphorsulfonic acid (CSA) as dopants. The PANI/CSA complex was prepared by using two different doping methods. (Unpublished data).

Blending. The blends were prepared with a corotating twin-screw mid-extruder. The screw speed was 60 rpm and temperature 200 °C. The mixing time was 3 min when preparing polyethylene blends. The content of the PANI complex in blends was 15 wt.%. The functionalized metallocene polyethylene content was 2 or 18 wt.%. The blend compositions are depicted with the sample designations in Table 6.

Table 6. Blend compositions for various samples.^{IV}

| Sample | Blend composition | Amount in the blend (wt.%) |
|---|---|----------------------------|
| PE/OH ₂ | LDPE/PE- <i>co</i> -OH | 98/2 |
| PE/COOH ₂ | LDPE/PE- <i>co</i> -COOH | 98/2 |
| PE/MAH ₂ | LDPE/PE- <i>g</i> -MAH | 98/2 |
| PE/OH ₁₈ | LDPE/PE- <i>co</i> -OH | 82/18 |
| PE/COOH ₁₈ | LDPE/PE- <i>co</i> -COOH | 82/18 |
| PE/MAH ₁₈ | LDPE/PE- <i>g</i> -MAH | 82/18 |
| ME/TSA | HDPE/(PANI/TSA) | 85/15 |
| PE/TSA | LDPE/(PANI/TSA) | 85/15 |
| PE/TSA/OH ₂ | LDPE/(PANI/TSA)/PE- <i>co</i> -OH | 83/15/2 |
| PE/TSA/COOH ₂ | LDPE/(PANI/TSA)/PE- <i>co</i> -COOH | 83/15/2 |
| PE/TSA/OH ₁₈ | LDPE/(PANI/TSA)/PE- <i>co</i> -OH | 67/15/18 |
| PE/TSA/COOH ₁₈ | LDPE/(PANI/TSA)/PE- <i>co</i> -COOH | 67/15/18 |
| PE/PSA | LDPE/(PANI/PSA) | 85/15 |
| PE/PSA/OH ₂ | LDPE/(PANI/PSA)/PE- <i>co</i> -OH | 83/15/2 |
| PE/PSA/COOH ₂ | LDPE/(PANI/PSA)/PE- <i>co</i> -COOH | 83/15/2 |
| PE/PSA/OH ₁₈ | LDPE/(PANI/PSA)/PE- <i>co</i> -OH | 67/15/18 |
| PE/PSA/COOH ₁₈ | LDPE/(PANI/PSA)/PE- <i>co</i> -COOH | 67/15/18 |
| PE/CSA ₁ | LDPE/(PANI/CSA ₁) | 85/15 |
| PE/CSA ₁ /OH ₂ | LDPE/(PANI/CSA ₁)/PE- <i>co</i> -OH | 83/15/2 |
| PE/CSA ₁ /COOH ₂ | LDPE/(PANI/CSA ₁)/PE- <i>co</i> -COOH | 83/15/2 |
| PE/CSA ₁ /MAH ₂ | LDPE/(PANI/CSA ₁)/PE- <i>g</i> -MAH | 83/15/2 |
| PE/CSA ₁ /ME ₂ | LDPE/(PANI/CSA ₁)/HDPE | 83/15/2 |
| PE/CSA ₁ /OH ₁₈ | LDPE/(PANI/CSA ₁)/PE- <i>co</i> -OH | 67/15/18 |
| PE/CSA ₁ /COOH ₁₈ | LDPE/(PANI/CSA ₁)/PE- <i>co</i> -COOH | 67/15/18 |
| PE/CSA ₁ /MAH ₁₈ | LDPE/(PANI/CSA ₁)/PE- <i>g</i> -MAH | 67/15/18 |
| PE/CSA ₁ /ME ₁₈ | LDPE/(PANI/CSA ₁)/HDPE | 67/15/18 |
| PE/CSA ₂ | LDPE/(PANI/CSA ₂) | 85/15 |
| PE/CSA ₂ /OH ₂ | LDPE/(PANI/CSA ₂)/PE- <i>co</i> -OH | 83/15/2 |
| PE/CSA ₂ /COOH ₂ | LDPE/(PANI/CSA ₂)/PE- <i>co</i> -COOH | 83/15/2 |
| PE/CSA ₂ /OH ₁₈ | LDPE/(PANI/CSA ₂)/PE- <i>co</i> -OH | 67/15/18 |
| PE/CSA ₂ /COOH ₁₈ | LDPE/(PANI/CSA ₂)/PE- <i>co</i> -COOH | 67/15/18 |

Characterization. Electrical conductivity was measured from extrudates by a four-probe method. Viscosity of the components was measured with a capillary rheometer. Tensile tests were done with an Instron testing machine. Thermal analyses with differential scanning calorimetry were performed to study the miscibility and interactions of the blend components. Morphology of the blends was characterized with SEM.

3.3 Conductivity of PANI blends

The conductivities of the blends were high for melt blending (Fig. 19). Blends with PANI/CSA complexes had the highest conductivities, even as good as the conductivity of the pure PANI/CSA complex (Fig. 18). Based on the conductivity results, PANI/CSA formed a continuous phase in the matrix polyethylene. The conductivities obtained in PANI/CSA₁ blends were slightly above electrostatic dissipation.

The addition of functionalized metallocene polyethylene did not disturb the percolation of the PANI complex, although the viscosity of the functionalized metallocene polyethylenes differs from that of the LDPE matrix. With metallocene polyethylene as the matrix and without a compatibilizer, the blend was an insulator even with 15 wt.% of the PANI complex. The viscosities of the LDPE and PANI/TSA complex were closer than the viscosities of the metallocene polyethylene and the PANI/TSA complex, which explains the conductivity obtained in the blends of LDPE and PANI complexes and not in the blends of metallocene polyethylene and PANI complexes.

In blends with the PANI/TSA complex, a small amount of functionalized metallocene polyethylene increased the conductivity. The PANI complex is probably located in the functionalized metallocene polyethylene phase or at the interphase, whereby double percolation occurs. With 18 wt.% of polyethylene with carboxylic acid functionality, conductivity dropped due to the unfavorable rheological properties of the blend components.

The conductivity of PANI/PSA blends, in contrast, did not change much with the addition of compatibilizers, and remained at the same level even at the higher content of compatibilizers. The PANI/PSA complex contains more functional groups able to form hydrogen bonds with the functionalized metallocene polyethylene, and these bonds compensate for the unfavorable rheological properties.

The same is seen with PANI/CSA₁ blends. Unless OH- or COOH-functionalized metallocene polyethylene was used, even 2 wt.% of unfunctionalized metallocene polyethylene in the blend disturbed the percolation of the PANI/CSA₁ complex, and the blend became an insulator. The PANI/CSA₂ complex, in turn, behaved more like the PANI/TSA complex: the conductivity of the PANI/CSA₂ blends increased with the addition of functionalized metallocene polyethylene, but was lower than

that of PANI/CSA1 blends, probably due to the different effect of the plasticizer on the PANI/CSA complexes.

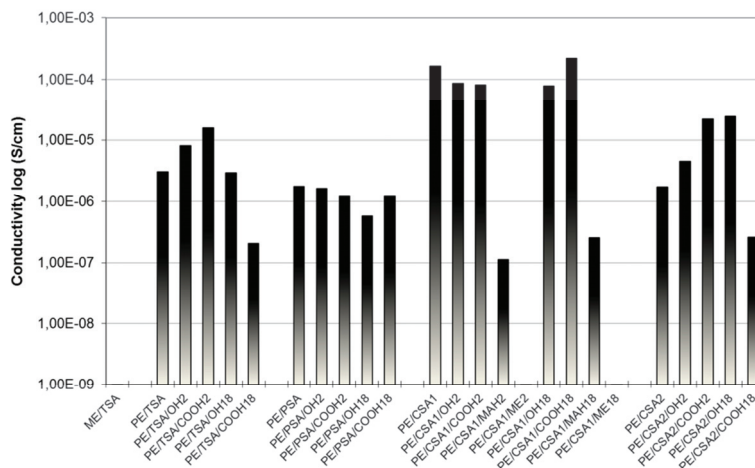


Figure 19. Conductivities of different PE/PANI blends. PANI complexes are denoted based on the dopants, toluenesulfonic acid (TSA), phenolsulfonic acid (PSA), and camphorsulfonic acid (CSA). Compatibilizers are denoted based on their functional group, hydroxyl group (OH) and carboxylic acid group (COOH), with the amount in the blend, 2 and 18 wt.%.^{IV}

3.4 Thermal Properties

The melting temperature of the polyethylene matrix was not affected by blending with the PANI complex, because polyethylene and PANI are not compatible. However, the crystallinity of the polyethylene matrix was decreased. Crystallinity of the polyethylene matrix was lowest if the blend contained PANI/CSA complexes. Free DBSA in the PANI/CSA1 complex was able to plasticize the matrix.

The melting temperatures of functionalized metallocene polyethylenes were shifted towards lower temperatures after the addition of the PANI complex. It can be assumed that the PANI complex is located in the same phase as the functionalized metallocene polyethylene, which partly explains the high conductivity of the blends with 2 wt.% of functionalized metallocene polyethylene. In the blends with 18 wt.% of functionalized metallocene polyethylene, the unfavorable rheological properties hinder the double percolation, as the LDPE matrix and the functionalized metallocene polyethylenes are immiscible as indicated by two distinct melting peaks in the DSC curve.

3.5 Mechanical Properties

The mechanical properties of polyethylene decreased with the addition of the PANI complexes (Fig. 20). Because the PANI complex is polar and the polyethylene matrix nonpolar, there is lack of adhesion between the different phases, and the mechanical properties of the polymer matrix are negatively affected by the PANI complex. The decrease in the crystallinity of the matrix LDPE negatively affects the mechanical properties as well.

Compared with the conventional Ziegler-Natta polyethylene LDPE, metallocene-catalyzed polyethylenes have better mechanical properties. [105,124] In the blends of LDPE matrix and functionalized metallocene polyethylene without PANI complex, tensile modulus and strain were improved after an 18 wt.% addition of functionalized metallocene polyethylene.

In the PANI/TSA and PANI/PSA blends, the tensile modulus increased with the addition of functionalized metallocene polyethylenes. A slight increase could be seen both in strength and strain. It is notable that when the PANI/PSA blend was compatibilized with 18 wt.% COOH-functionalized polyethylene, the mechanical properties were greatly improved without a reduction in the electrical conductivity of the blend.

Tensile modulus and strength were worse in the PANI/CSA1 blends than in the other PANI complex blends. The PANI/CSA complexes were post-plasticized with ZnO₂ and DBSA, and free DBSA most probably migrated into the matrix and functionalized polyethylene phases and plasticized them as well. [127] The strain of the blends increased due to the plasticization effect. Better mechanical properties were achieved in PANI/CSA1 blends with MAH-functionalized polyethylene as compatibilizer, where the free plasticizer forms covalent bonds with MAH-functionalized polyethylene, but after that the conductivities decreased.

The plasticizer is evidently better bonded in the PANI/CSA2 complex than in the PANI/CSA1 complex, and the mechanical properties of the blend are therefore clearly improved after the addition of functionalized polyethylenes. With 18 wt.% OH-functionalized polyethylene as compatibilizer, both modulus and strength were improved over that of the PANI/CSA1 blends.

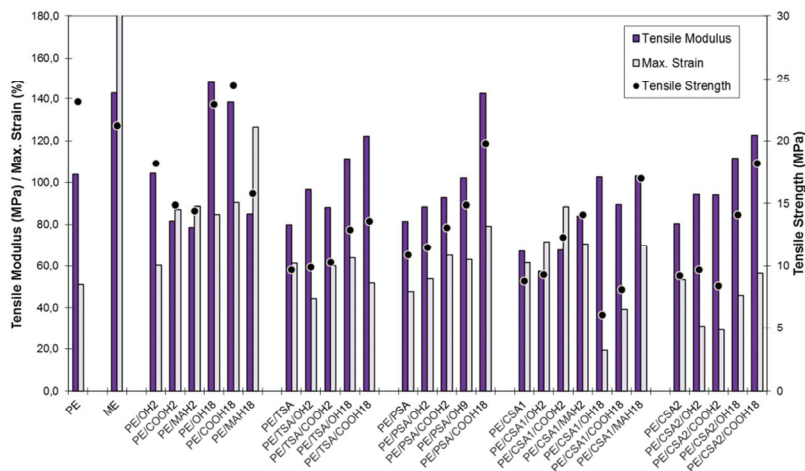


Figure 20. Mechanical properties of different PE/PANI blends. PANI complexes are denoted based on the dopants, toluenesulfonic acid (TSA), phenolsulfonic acid (PSA), and camphorsulfonic acid (CSA). Compatibilizers are denoted based on their functional group, hydroxyl group (OH), carboxylic acid group (COOH), and maleic anhydride (MAH), with the amount in the blend, 2 and 18 wt.%.^{IV}

3.6 Morphology of PANI blends

For the conductivity, PANI has to form a continuous phase in the blends. Differences in conductivity are explained by the morphological structure observed in SEM images. In the blends without functionalized polyethylene, the PANI complex was mostly in the dispersed phase and the conductivity of the blends was weaker. In the blends with functional polyethylene, the network structure can be seen (Fig. 21). The network structures are finer in the PANI/PSA blends than in the PANI/TSA blends, explaining the differences in the conductivities of the blends. In the blends with MAH-functionalized polyethylene, the same kind of dispersion or network structure of the PANI complex is not seen, and the fracture surface is very smooth. In the blends containing metallocene polyethylene without functionalities, the surface is very rough and there is no adhesion between the two phases.

Figure 22 shows the fracture surface of a tensile test specimen of the PANI/CSA1 blend after the test. The lamellar structure of phases, which is formed during the tensile test, is clearly visible. The same kind of lamellar structure is seen in the blends with compatibilizers. Mechanical properties are greatly affected by the adhesion of the lamellar phases.

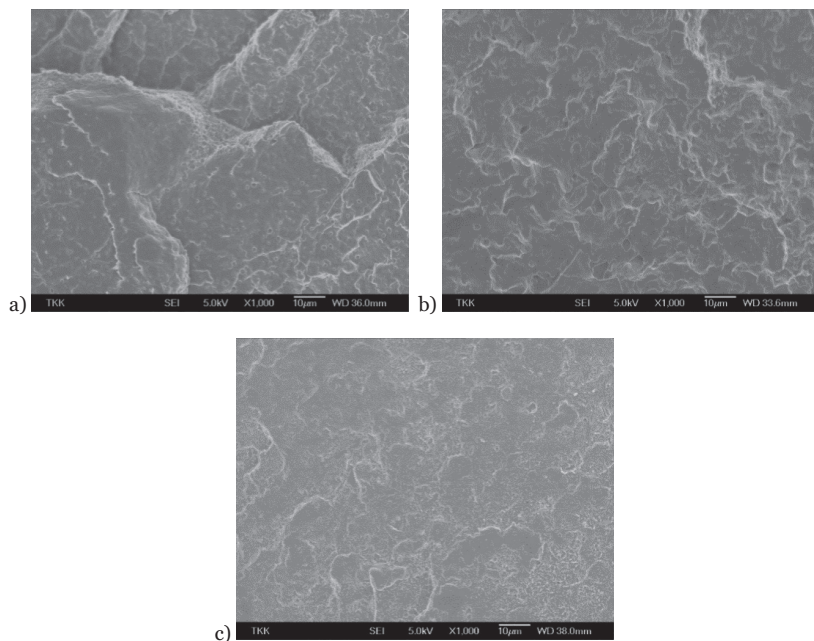


Figure 21. SEM images of PE/(PANI/TSA) blends with a) no compatibilizer, b) 2 wt.% OH-functionalized PE, and c) 18 wt.% OH-functionalized PE.^{IV}

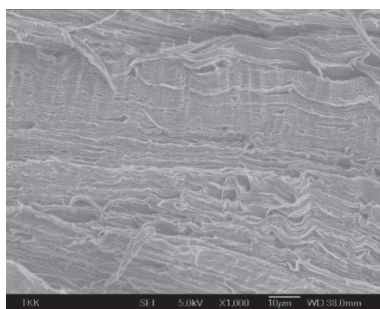


Figure 22. SEM image of a PANI/CSA1 blend sample after a tensile test.^{IV}

4. Proton conductive poly(ethylene-co-styrene) membranes

4.1 The benefit of using metallocene polymers as a proton conductive material

Solution casting is a widely used processing method for polymeric electrolytes. However, it does not give any processing benefits over hydrogels or liquid electrolytes that cannot be melt processed. Solid thermoplastic electrolytes can be melt processed. The benefits of melt processing are clear where time and materials are concerned. Solution casting can take days due to the evaporation of solvents, whereas melt processing takes only minutes. [81,128] In melt processing, there are no additional solvents, which can affect the morphology of the membranes, need to be removed, and can be very harmful or toxic.

A novel approach to prepare proton-conducting polymer materials is to use a metallocene polymerized copolymer. Without fluoropolymer, the metallocene polymer is environmentally friendlier. The advantage of using metallocene polymers is the ability to tailor various properties, although fluoropolymers have good chemical and mechanical strength. With metallocene polymerization, it is possible to use ethylene as a monomer and styrene as a comonomer. Even though the chemical and mechanical strength of polyethylene is not as good as those of fluoropolymers, it fares well in comparison with polystyrene. Metallocene catalysts allow a direct copolymerization of functional monomers with an even comonomer distribution throughout the whole polymer chain. [124] Therefore, it is possible to prepare random ethylene/styrene copolymers without polystyrene blocks, i.e. small controlled structures exhibiting melt processability. After the sulfonation of the phenyl rings, the copolymer becomes a proton conductor.

4.2 Material preparations and characterizations

Polymerization. The ethylene/styrene copolymer was synthesized with a metallocene catalyst. [129] The residues of polyethylene and polystyrene homopolymers were removed before further processing.

Membrane fabrications. Membranes were prepared by hot-pressing copolymer into films at 150 °C and a 150 kN pressure for 3 min. To strengthen the copolymer membrane, glassfiber tissue instead of individual glassfibers, was used to form an even distribution of glassfibers in the composite membrane. To keep the glassfiber tissue as intact as possible, very low pressure and a long melting time were applied, and the glassfiber tissue was covered on both sides with the copolymer film to properly wet the glassfibers. The composite membranes were prepared by placing the glassfiber tissue between two copolymer films and melted at 150 °C for 10 min at a light pressure of 30 kN.

Sulfonation reaction. Sulfonation was carried out with chlorosulfonic acid in dichloroethane (DCE). The membranes were soaked in the acid solution and the volume of solution was large enough to keep the concentration of the solution constant during the sulfonation reaction. Two acid concentrations were tested: a weak 0.5 M solution and a strong 1.0 M solution. The reaction was allowed to proceed for 1-4 h at 0 °C and the membranes were washed after the sulfonation reaction. The pristine glassfiber tissue was subjected to sulfonation processes in order to see if the sulfonation reaction affects the glassfiber tissue.

Characterizations. The molecular structure of the copolymer was determined with nuclear magnetic resonance (NMR) and thermal properties with differential scanning calorimetry (DSC). Water sorption was determined by boiling the sulfonated membranes for one hour in deionized water. Water uptake was determined according to equation 5:

$$\text{water uptake} = \frac{W_{\text{wet}} - W_{\text{dry}}}{W_{\text{dry}}} \quad (5)$$

where w_{wet} is the mass of the wet sample and w_{dry} is the mass of the dried sample.

Ion exchange capacity (IEC, meq/g) was measured by back titration. IEC was calculated from equation 6:

$$\text{IEC} = \frac{n_1 - n_0}{m_{\text{dry}}} \quad (6)$$

where n_1 is moles of hydroxide ions originally present, n_0 moles of hydrochloric acid consumed, and m_{dry} the mass of the dried sample.

Ionic conductivities were recorded by impedance spectroscopy. Before the measurement the membranes were equilibrated with water vapor in a sealed vessel for a minimum of 3 days, after which the proton conductivity was determined at 25 °C at 100% relative humidity. Mechanical properties of the membranes were analyzed with dynamic mechanical analysis (DMA).

4.3 Structure and morphology of copolymer and membranes

Based on the ^{13}C -NMR and DSC results, the sulfonic acid groups were evenly distributed along the membranes. The microstructure of the synthesized copolymer was determined from the ^{13}C -NMR spectra, and the nearly alternating structure with 47 mol-% of styrene was verified. A clear sign of glass transition temperature was found at ~ 30 °C, which correlates well with the previous results where alternating ethylene/styrene copolymers were synthesized. [130-132] Based on these results, there were no large polystyrene and polyethylene blocks in the copolymer, as the styrene/ethylene molar ratio was nearly 1:1.

The movements of polymer chains during the melt state are limited compared with the solvate state. Therefore, large styrene and ethylene domains cannot form during melt processing, even though the melt processing time was several minutes. During the sulfonation step, the membrane was swollen and polymer chains could rearrange themselves towards a lower thermodynamic state. The phase separation could occur due to the large value of the solubility parameter between sulfonated and non-sulfonated domains, but not to the same extent as in the solvate state or without large blocks of polyethylene and polystyrene.

Optical microscope images show (Fig. 23) that the pristine glassfiber tissue after the sulfonation reaction and the glassfiber tissue after hot-pressing with a copolymer stayed almost intact. After the sulfonation reaction of the reinforced membrane, the glassfiber tissue was covered by the copolymer without air pockets in the membranes.

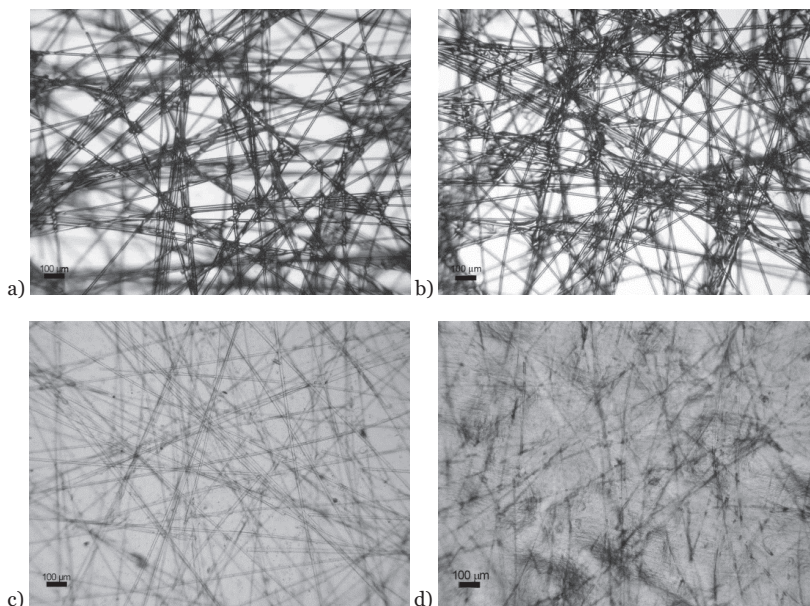


Figure 23. Optical microscopy images of a) pristine glassfiber tissue, b) sulfonated glassfiber tissue, c) composite membrane before sulfonation, and d) composite membrane after sulfonation.^v

4.4 Effect of sulfonation

A high sulfonation degree was achieved due to the high amount of styrene units in the copolymer and therefore water uptakes were high. Concentration of the sulfonation solution was a significant parameter for preparing the membranes with sufficient properties. The solvent, DCE, softened the membranes but did not totally dissolve them when chlorosulfonic acid was present. Chlorosulfonic acid penetrated into the swollen membrane and sulfonated the phenyl rings. At the same time, crosslinks between sulfonic acid groups formed, which prevented the membrane from dissolving. By using a longer sulfonation reaction time, crosslinking increased and water uptake decreased. Use of a stronger acid concentration increased the amount of crosslinks, and decreased the water uptake even more.

4.4.1 Ion exchange capacity

Ion exchange capacity (IEC) depicted the actual amount of free sulfonic acid groups in the membrane and the effect of crosslinking (Fig. 24). IEC decreased as the water uptake decreased, but not to the same extent (Fig. 25). With lower chlorosulfonic acid concentration, 0.5 mol/dm^3 , after a 1 h

reaction time, water uptake was very high, but IEC was sufficiently low. With a lower acid concentration, DCE could swell the membrane more efficiently, but sulfonation and crosslinking reactions were slower. When the reaction time was extended, sulfonation reaction continued and IEC first increased and then decreased as the crosslinking increased. At a higher chlorosulfonic acid concentration, 1.0 mol/dm³, high IEC was obtained with a much lower water uptake value. By extending the reaction time with a higher acid concentration, IEC decreased rapidly, as the reactions were faster.

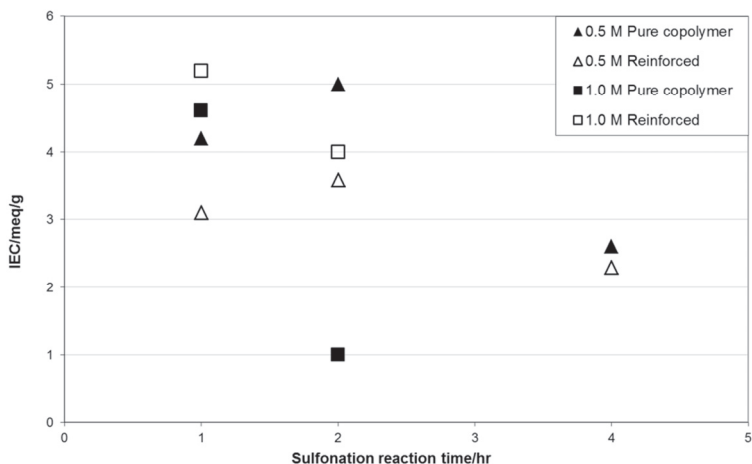


Figure 24. Ion exchange capacity of the membranes. 0.5 M denotes a weaker sulfonation solution and 1.0 M a stronger sulfonation solution.^v

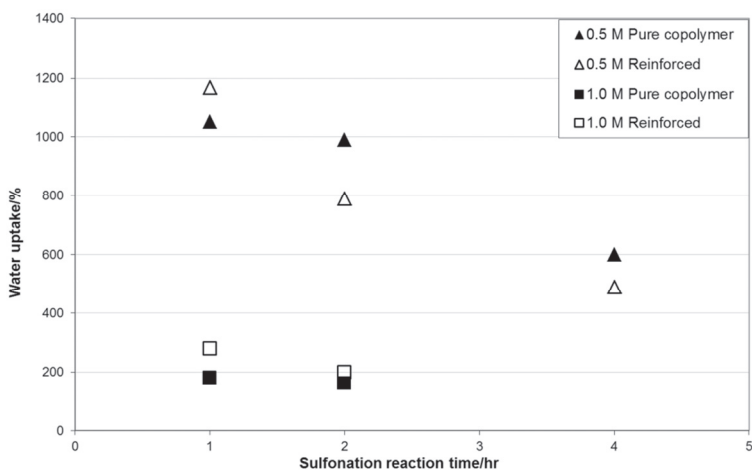


Figure 25. Water uptake of the membranes. 0.5 M denotes a weaker sulfonation solution and 1.0 M a stronger sulfonation solution.^v

The glassfiber tissue affected the properties of the sulfonated membranes only indirectly, hindering the crosslinking of the copolymer and providing mechanical support and strength for the membrane.

In the case of the lower chlorosulfonic acid concentration, DCE could swell the membrane more efficiently and acid penetrated through the membrane more easily without the glassfiber tissue. Therefore, sulfonation reaction was more effective and the pure copolymer membranes without reinforcement had higher IEC at all sulfonation reaction times (Fig. 24). However, after 1 h reaction time in a weaker sulfonation solution, the pure copolymer membrane had a lower water uptake than the reinforced membrane (Fig. 25). With a short sulfonation reaction time and a lower acid concentration, there was less crosslinking due to the slower reaction rate. The swollen membrane structure could be broken down by water and the membrane could retain less water. When the membrane was reinforced, the glassfiber tissue supported the membrane structure and maintained the high water uptake though IEC was lower compared with IEC of the pure copolymer membrane. When sulfonation reaction time was extended, crosslinking increased in the pure copolymer membrane and the membrane was more stable.

In the case of a higher chlorosulfonic acid concentration, 1.0 mol/dm³, both reactions, sulfonation and crosslinking, took place more effectively than in the weaker solution. The glassfiber tissue acted as a barrier to crosslinking. Therefore, there were more free sulfonic acid groups in the reinforced membranes and water uptake and IEC were higher in reinforced membranes at all sulfonation reaction times.

4.4.2 Proton conductivity

Proton conductivity of the membranes depended on the water uptake, i.e. the mechanical properties of the membranes and the amount of sulfonic acid groups in the membranes. All the measured conductivities were good (Fig. 26), mostly above 50 mS/cm. These conductivities were at the same level as the conductivities of the commercial Nafion and radiation-grafted PVDF membranes under the same conditions. [133] The long sulfonation time increased the crosslinking and reduced the amount of free sulfonic acid groups in the membranes, and conductivities decreased. All the reinforced membranes were mechanically good enough so that the conductivity measurements could be performed. However, the membranes

without glassfiber tissue were mostly too weak to hold the contact pressure created by the measuring electrodes.

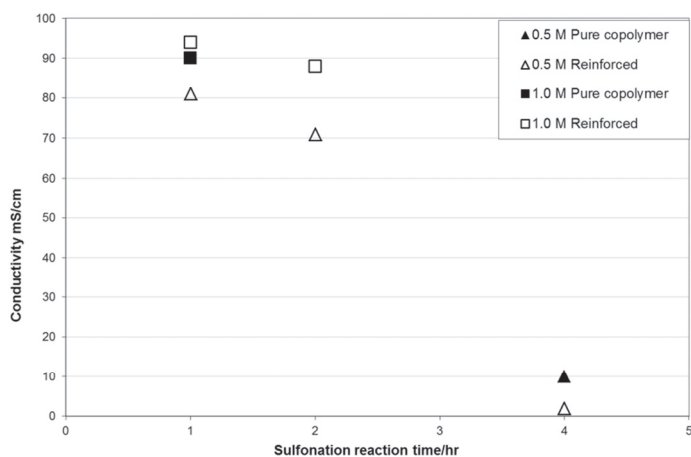


Figure 26. Proton conductivity of the membranes. 0.5 M denotes a weaker sulfonation solution and 1.0 M a stronger sulfonation solution.^V

4.4.3 Strength of membranes

Mechanical properties of the membranes depended on the measuring conditions. For the reinforced copolymer, T_g was at the same temperature as for the pure copolymer, but the collapse of the mechanical strength of the membrane shifted to a higher temperature. The crosslinks in the sulfonated membrane shifted the T_g to a higher temperature and inhibited the collapse of mechanical strength. In DMA measurement conditions, at air humidity, crosslinking affected the mechanical properties more than the glassfiber tissue. The storage modulus and the loss modulus were higher in the sulfonated membranes without glassfiber tissue. However, the effect of moisture on the mechanical properties emphasizes the importance of reinforcement at a high sulfonation level, which is required for good proton conductivity.

5. Conclusions

The conductivity in polymeric materials can form at least in three different ways. Depending on the electrical conductivity, charge carriers, electrons or ions, can move along the polymer chains as in PANI, along the surface as through carbon nanotubes in composites, or in the medium, as moisture in the proton conductive membranes. One of the challenges in each of these entities is how to maintain good conductivity with good mechanical properties.

Even though conductivities are formed differently in various conductive polymeric materials, similar solutions can be applied to improve both conductivity and mechanical properties. Good dispersion of CNTs was attained by using *in situ* polymerization techniques. With the use of polymers prepared with metallocene catalysts it was possible to efficiently compatibilize PANI/PE blends and even form ionically conductive material.

The obtained conductivities of CNTs composites were not at the highest level with similar CNTs contents reported in the literature. However, one of the main discoveries of the *in situ* polymerization of CNTs was to recognize to which extent MWCNTs are able to influence the *in situ* polymerizations by affecting the molecular weight of a polymer. Based on the quality and the amount of CNTs as well as on the compatibility of CNT and the monomer, the molecular weight of a polymer can be tailored. At the same time, stable dispersion of an individual CNT was obtained. Therefore, it was possible to use a CNT composite as a masterbatch and utilize conventional polymer blending techniques. Based on the possibility to tailor the molecular weight, the improvements of the mechanical properties of the *in situ* polymerized composites were not solely due to the presence of CNTs but also to the increase in the molecular weight of the polymer.

A novel approach was to use hydroxyl and carboxylic acid functionalized metallocene copolymers as compatibilizers in PANI/PE blends. The conductivity of the PANI/PE blend was as good as that of the pure PANI complex, and increasing the conductivity to a higher level would require the development of the PANI complex. However, the mechanical properties of the PANI/PE blends were clearly improved after the addition of

metallocene polyethylene. Literature review did not reveal similar results. According to the literature, the conductivity of PANI could be transferred to a blend, but simultaneously the mechanical properties were worsened as compared with a matrix polymer.

In addition to compatibilization, a novel approach was to use metallocene polyethylenes as a proton-conducting material. Because of the stereospecific structure, sulfonic acid groups were evenly distributed through the membrane of the ethylene/styrene copolymer. With a large number of sulfonic acid groups, good proton conductivity was obtained with high ion exchange capacity. Even though the stability of the membranes was not as good as the stability of fluoropolymers that are used in fuel cells, the obtained conductivities were competitive in applications like sensors and actuators.

Both the MWCNT composites and the PANI blends had good electronic conductivities. The obtained conductivities were almost at the EMI level in both cases, above 10^{-4} S/cm. However, the stability of conductivity in MWCNT composites is better than in PANI blends. Due to the chemical stability of MWCNTs, MWCNTs tolerate stronger thermal treatments compared with the PANI complex, in which dopant is not covalently bonded to PANI. Because of the differences in conductivity measurement, electronic and ionic conductivities are not comparable. However, the proton conductivity of sulfonated ethylene/styrene copolymers was also good; the highest value was almost 10^{-2} S/cm.

For future research, it would be interesting to use the results obtained in this study to combine two different materials with electronic conductivities. The PANI/CNT composite, obtained with *in situ* polymerization of aniline in the presence of CNTs and further doping, could be used as a masterbatch. The PANI/CNT masterbatch would give exceptional properties for a composite. CNT would contribute to electrical conductivity together with PANI, but at the same time, CNTs would improve the stability of PANI complex both in thermal processing and electrical conductivity. The PANI complex in turn would serve as the proper medium for electrons to move from tube to tube.

References

1. Li Y., Moon K., Wong C.P., Electronics without lead, *Science* **308** (2005) 1419-1420.
2. Rybak A., Boiteux G., Melis F., Seytre G., Conductive polymer composites based on metallic nanofiller as smart materials for current limiting devices, *Compos. Sci. Technol.* **70** (2010) 410-416.
3. Zhang R., Moon K., Lin W., Agar J.C., Wong C., A simple, low-cost approach to prepare flexible highly conductive polymer composites by in situ reduction of silver carboxylate for flexible electronic applications, *Compos. Sci. Technol.* **71** (2011) 528-534.
4. Markarian J., New developments in antistatic and conductive additives, *Plastics, Additives and Compounding* **10** (2008) 22-25.
5. Rupprecht L., editor, *Conductive polymers and plastics in industrial applications*, William Andrew Publishing, Norwich, 1999, 285 pp.
6. MacDiarmid A.G., Polyaniline and polypyrrole: Where are we headed?, *Synth. Met.* **84** (1997) 27-34.
7. Heeger A.J., Semiconducting and metallic polymers: the fourth generation of polymeric materials, *Synth. Met.* **125** (2001) 23-42.
8. Gray F.M., *Polymer electrolytes, RCS Materials Monographs*, The Royal Society of Chemistry, Cambridge, 1997, 175 pp.
9. Rikukawa M., Sanui K., Proton-conducting polymer electrolyte membranes based on hydrocarbon polymers, *Prog. Polym. Sci.* **25** (2000) 1463-1502.
10. Scher H., Zallen R., Critical density in percolation processes, *J. Chem. Phys.* **53** (1970) 3759-3761.
11. Dudić D., Škipina B., Dojčilović J., Novaković L., Kostoski D., Effects of charge trapping on the electrical conductivity of low-density polyethylene-carbon black composites, *J. Appl. Polym. Sci.* **121** (2011) 138-143.
12. Li F., Qi L., Yang J., Xu M., Luo X., Ma D., Polyurethane/conducting carbon black composites: Structure, electric conductivity, strain recovery behavior, and their relationships, *J. Appl. Polym. Sci.* **75** (2000) 68-77.
13. Hermant M.C., Smeets N., Van Hal R., Meuldijk J., Heuts H., Klumperman B., Van Herk A., Koning C., Influence of the molecular weight distribution on the percolation threshold of carbon nanotube - polystyrene and polymethylmethacrylate composites, *e-Polymers* **022** (2009) 1-13.

14. Bryning M.B., Islam M.F., Kikkawa J.M., Yodh A.G., Very low conductivity threshold in bulk isotropic single-walled carbon nanotube-epoxy composites, *Adv. Mater.* **17** (2005) 1186-1191.
15. Sawada I., Fachrul R., Ito T., Ohmukai Y., Maruyama T., Matsuyama H., Development of a hydrophilic polymer membrane containing silver nanoparticles with both organic antifouling and antibacterial properties, *J. Membr. Sci.* **387-388** (2012) 1-6.
16. Dresselhaus M.S., Dresselhaus G., Pimenta M., The remarkable properties of carbon nanotubes as nanoclusters, *Eur. Phys. J. D* **9** (1999) 69-75.
17. Valentin N.P., Carbon nanotubes: properties and application, *Mater. Sci. Eng., R* **43** (2004) 61-102.
18. Jorio A., Dresselhaus G., Dresselhaus M.S., editors, *Carbon nanotubes: Advanced topics in the synthesis, structure, properties and applications (Topics in applied physics)*, Springer, Berlin, 2008, 720 pp.
19. Li Q.W., Li Y., Zhang X.F., Chikkannanavar S.B., Zhao Y.H., Dangelewicz A.M., Zheng L.X., Doorn S.K., Jia Q.X., Peterson D.E., Arendt P.N., Zhu Y.T., Structure-dependent electrical properties of carbon nanotube fibers, *Adv. Mater.* **19** (2007) 3358-3363.
20. Gau C., Kuo C.Y., Ko H.S., Electron tunneling in carbon nanotube composites, *Nanotechnology* **20** (2009) 395705.
21. Gábor T., Aranyi D., Papp K., Kármán F.H., Kálmán E., Dispersibility of carbon nanotubes, *Materials Science Forum* **537-538** (2007) 161-168.
22. Peng X., Wong S.S., Functional covalent chemistry of carbon nanotube surfaces, *Adv. Mater.* **21** (2009) 625-642.
23. Tchoul M.N., Ford W.T., Lolli G., Resasco D.E., Arepalli S., Effect of mild nitric acid oxidation on dispersability, size, and structure of single-walled carbon nanotubes, *Chem. Mater.* **19** (2007) 5765-5772.
24. Yu H., Jin Y., Peng F., Wang H., Yang J., Kinetically controlled side-wall functionalization of carbon nanotubes by nitric acid oxidation, *J. Phys. Chem. C* **112** (2008) 6758-6763.
25. Tasis D., Tagmatarchis N., Bianco A., Prato M., Chemistry of carbon nanotubes, *Chem. Rev.* **106** (2006) 1105-1136.
26. Callister W.D., *Materials science and engineering: An introduction*, 7th Revised ed., John Wiley and Sons Inc., New York, 2007, 832 pp.
27. Moniruzzaman M., Winey K.I., Polymer nanocomposites containing carbon nanotubes, *Macromolecules* **39** (2006) 5194-5205.
28. Isayev A.I., Kumar R., Lewis T.M., Ultrasound assisted twin screw extrusion of polymer-nanocomposites containing carbon nanotubes, *Polymer* **50** (2009) 250-260.

29. Lin B., Sundararaj U., Pötschke P., Melt mixing of polycarbonate with multi-walled carbon nanotubes in miniature mixers, *Macromol. Mater. Eng.* **291** (2006) 227-238.
30. Mičušík M., Omastová M., Krupa I., Prokeš J., Pissis P., Logakis E., Pandis C., Pötschke P., Pionteck J., A comparative study on the electrical and mechanical behaviour of multi-walled carbon nanotube composites prepared by diluting a masterbatch with various types of polypropylenes, *J. Appl. Polym. Sci.* **113** (2009) 2536-2551.
31. Kim S., Choi H., Hong S., Bulk polymerized polystyrene in the presence of multiwalled carbon nanotubes, *Colloid. Polym. Sci.* **285** (2007) 593-598.
32. Xia H., Qiu G., Wang Q., Polymer/carbon nanotube composite emulsion prepared through ultrasonically assisted in situ emulsion polymerization, *J. Appl. Polym. Sci.* **100** (2006) 3123-3130.
33. Wiemann K., Kaminsky W., Gojny F.H., Schulte K., Synthesis and properties of syndiotactic poly(propylene)/carbon nanofiber and nanotube composites prepared by in situ polymerization with metallocene/MAO catalysts, *Macromol. Chem. Phys.* **206** (2005) 1472-1478.
34. Gorga R.E., Cohen R.E., Toughness enhancements in poly(methyl methacrylate) by addition of oriented multiwall carbon nanotubes, *J. Polym. Sci., Part B: Polym. Phys.* **42** (2004) 2690-2702.
35. Feldman A.Y., Larin B., Berestetsky N., Marom G., Weinberg A., Microbeam WAXD study of orientated crystalline arrays in carbon fiber/CNT – nylon 66 extruded/drawn composites, *J. Macromol. Sci., Part B: Phys.* **46** (2007) 111-117.
36. Salalha W., Dror Y., Khalfin R.L., Cohen Y., Yarin A.L., Zussman E., Single-walled carbon nanotubes embedded in oriented polymeric nanofibers by electrospinning, *Langmuir* **20** (2004) 9852-9855.
37. Du F., Fischer J.E., Winey K.I., Coagulation method for preparing single-walled carbon nanotube/poly(methyl methacrylate) composites and their modulus, electrical conductivity, and thermal stability, *J. Polym. Sci., Part B: Polym. Phys.* **41** (2003) 3333-3338.
38. Kharchenko S.B., Douglas J.F., Obrzut J., Grulke E.A., Migler K.B., Flow-induced properties of nanotube-filled polymer materials, *Nat. Mater.* **3** (2004) 564-568.
39. Bauhofer W., Kovacs J.Z., A review and analysis of electrical percolation in carbon nanotube polymer composites, *Compos. Sci. Technol.* **69** (2009) 1486-1498.
40. Ji L., Stevens M.M., Zhu Y., Gong Q., Wu J., Liang J., Preparation and properties of multi-walled carbon nanotube/carbon/polystyrene composites, *Carbon* **47** (2009) 2733-2741.
41. Khan M.U., Gomes V.G., Altarawneh I.S., Synthesizing polystyrene/carbon nanotube composites by emulsion polymerization with non-covalent and covalent functionalization, *Carbon* **48** (2010) 2925-2933.

42. Wu H., Qiu X., Cao W., Lin Y., Cai R., Qian S., Polymer-wrapped multiwalled carbon nanotubes synthesized via microwave-assisted in situ emulsion polymerization and their optical limiting properties, *Carbon* **45** (2007) 2866-2872.
43. Ham H.T., Choi Y.S., Chee M.G., Chung I.J., Singlewall carbon nanotubes covered with polystyrene nanoparticles by *in-situ* miniemulsion polymerization, *J. Polym. Sci., Part A: Polym. Chem.* **44** (2006) 573-584.
44. Zhang W., Yang M.J., Dispersion of carbon nanotubes in polymer matrix by in-situ emulsion polymerization, *J. Mater. Sci.* **39** (2004) 4921-4922.
45. Matarredona O., Rhoads H., Li Z., Harwell J.H., Balzano L., Resasco D.E., Dispersion of single-walled carbon nanotubes in aqueous solutions of the anionic surfactant NaDDBS, *J. Phys. Chem. B* **107** (2003) 13357-13367.
46. Orel Z.C., Gunde M.K., Spectrally selective paint coatings: Preparation and characterization, *Sol. Energy Mater. Sol. Cells* **68** (2001) 337-353.
47. Ports B.F., Weiss R.A., One-step melt extrusion process for preparing polyolefin/clay nanocomposites using natural montmorillonite, *Ind. Eng. Chem. Res.* **49** (2010) 11896-11905.
48. Jin S.H., Kang C.H., Yoon K.H., Bang D.S., Park Y., Effect of compatibilizer on morphology, thermal, and rheological properties of polypropylene/functionalized multi-walled carbon nanotubes composite, *J. Appl. Polym. Sci.* **111** (2009) 1028-1033.
49. Jordhamo G.M., Manson J.A., Sperling L.H., Phase continuity and inversion in polymer blends and simultaneous interpenetrating networks, *Polym. Eng. Sci.* **26** (1986) 517-524.
50. Meincke O., Kaempfer D., Weickmann H., Friedrich C., Vathauer M., Warth H., Mechanical properties and electrical conductivity of carbon-nanotube filled polyamide-6 and its blends with acrylonitrile/butadiene/styrene, *Polymer* **45** (2004) 739-748.
51. Pötschke P., Bhattacharyya A.R., Janke A., Morphology and electrical resistivity of melt mixed blends of polyethylene and carbon nanotube filled polycarbonate, *Polymer* **44** (2003) 8061-8069.
52. Kang E.T., Neoh K.G., Tan K.L., Polyaniline: A polymer with many interesting intrinsic redox states, *Prog. Polym. Sci.* **23** (1998) 277-324.
53. Tishchenko G.A., Dybal J., Stejskal J., Kúdela V., Bleha M., Rosova E.Y., Elyashevich G.K., Electrical resistance and diffusion permeability of microporous polyethylene membranes modified with polypyrrole and polyaniline in solutions of electrolytes, *J. Membr. Sci.* **196** (2002) 279-287.
54. Jin Z., Su Y., Duan Y., Development of a polyaniline-based optical ammonia sensor, *Sens. Actuators, B* **72** (2001) 75-79.
55. Andersson P., Berggren M., Kugler T., Switchable optical polarizer based on electrochromism in stretch-aligned polyaniline, *Appl. Phys. Lett.* **83** (2003) 1307-1309.

56. Ikkala O.T., Pietilä L.-O., Passiniemi P., Vikki T., Österholm H., Ahjopalo L., Österholm J.-E., Processible polyaniline complexes due to molecular recognition: Supramolecular structures based on hydrogen bonding and phenyl stacking, *Synth. Met.* **84** (1997) 55-58.
57. MacDiarmid A.G., Zhou Y., Feng J., Oligomers and isomers: new horizons in poly-anilines, *Synth. Met.* **100** (1999) 131-140.
58. Li J., Fang K., Qiu H., Li S., Mao W., Micromorphology and electrical property of the HCl-doped and DBSA-doped polyanilines, *Synth. Met.* **142** (2004) 107-111.
59. Krinichnyi V.I., Chemerisov S.D., Lebedev Y.S., EPR and charge-transport studies of polyaniline, *Phys. Rev. B* **55** (1997) 16233-16244.
60. Novak M., Kokanović I., Babić D., Baćani M., Tonejc A., Variable-range-hopping exponents 1/2, 2/5 and 1/4 in HCl-doped polyaniline pellets, *Synth. Met.* **159** (2009) 649-653.
61. MacDiarmid A.G., Epstein A.J., Secondary doping in polyaniline, *Synth. Met.* **69** (1995) 85-92.
62. Dahman S.J., The effect of co-dopants on the processability of intrinsically conducting polymers, *Polym. Eng. Sci.* **39** (1999) 2181-2188.
63. Cao Y., Smith P., Heeger A.J., Counter-ion induced processibility of conducting polyaniline and of conducting polyblends of polyaniline in bulk polymers, *Synth. Met.* **48** (1992) 91-97.
64. Virtanen E., Laakso J., Ruohonen H., Väkiparta K., Järvinen H., Jussila M., Passiniemi P., Österholm J.-E., Electrically conductive compositions based on processible polyanilines — PANEPOL™, *Synth. Met.* **84** (1997) 113-114.
65. Yang J.P., Rannou P., Planès J., Proñ A., Nechtschein M., Preparation of low density polyethylene-based polyaniline conducting polymer composites with low percolation threshold via extrusion, *Synth. Met.* **93** (1998) 169-173.
66. Utracki L.A., editor, *Polymer blends handbook*, Kluwer Academic, Boston, 2002, 1442 pp.
67. Xie H., Ma Y., Guo J., Secondary doping phenomena of two conductive polyaniline composites, *Synth. Met.* **123** (2001) 47-52.
68. Valenciano G.R., Job A.E., Mattoso L.H.C., Improved conductivity of films of ultra high molecular weight polyethylene and polyaniline blends prepared from an m-cresol/decaline mixture, *Polymer* **41** (2000) 4757-4760.
69. Zhang Q.H., Gao J., Wang X.H., Chen D.J., Jing X.B., Phase separation of polyaniline blends with thermoplastic polymers, *Synth. Met.* **135-136** (2003) 479-480.
70. Smitha B., Sridhar S., Khan A.A., Solid polymer electrolyte membranes for fuel cell applications—a review, *J. Membr. Sci.* **259** (2005) 10-26.

71. DeLuca N.W., Elabd Y.A., Polymer electrolyte membranes for the direct methanol fuel cell: A review, *J. Polym. Sci., Part B: Polym. Phys.* **44** (2006) 2201-2225.
72. Hickner M.A., Fujimoto C.H., Cornelius C.J., Transport in sulfonated poly(phenylene)s: Proton conductivity, permeability, and the state of water, *Polymer* **47** (2006) 4238-4244.
73. Kreuer K.D., Fuchs A., Ise M., Spaeth M., Maier J., Imidazole and pyrazole-based proton conducting polymers and liquids, *Electrochim. Acta* **43** (1998) 1281-1288.
74. Pu H., Liu Q., Qiao L., Yang Z., Studies on proton conductivity of acid doped polybenzimidazole/polyimide and polybenzimidazole/polyvinylpyrrolidone blends, *Polym. Eng. Sci.* **45** (2005) 1395-1400.
75. Pisani L., Valentini M., Hofmann D.H., Kuleshova L.N., D'Aguanno B., An analytical model for the conductivity of polymeric sulfonated membranes, *Solid State Ionics* **179** (2008) 465-476.
76. Selvan M.E., Keffer D.J., Cui S., Reactive molecular dynamics study of proton transport in polymer electrolyte membranes, *J. Phys. Chem. C* **115** (2011) 18835-18846.
77. Park C.H., Lee C.H., Sohn J., Park H.B., Guiver M.D., Lee Y.M., Phase separation and water channel formation in sulfonated block copolyimide, *J. Phys. Chem. B* **114** (2010) 12036-12045.
78. Münch W., Kreuer K.-D., Silvestri W., Maier J., Seifert G., The diffusion mechanism of an excess proton in imidazole molecule chains: first results of an ab initio molecular dynamics study, *Solid State Ionics* **145** (2001) 437-443.
79. Han M.J., Park J.H., Lee J.Y., Jho J.Y., Ionic polymer-metal composite actuators employing radiation-grafted fluoropolymers as ion-exchange membranes, *Macromol. Rapid Commun.* **27** (2006) 219-222.
80. Lee D.Y., Heo S., Kim K.J., Kim D., Lee M.H., Lee S.J., Electrically controllable biomimetic actuators made with multiwalled carbon nanotube (MWNT) loaded ionomeric nanocomposites, *Key Engineering Materials* **284-286** (2005) 733-736.
81. Wang X., Oh I., Cheng T., Electro-active polymer actuators employing sulfonated poly(styrene-ran-ethylene) as ionic membranes, *Polym. Int.* **59** (2010) 305-312.
82. Pantelić N., Andria S.E., Heineman W.R., Seliskar C.J., Characterization of partially sulfonated polystyrene-*block*-poly(ethylene-ran-butylene)-*block*-polystyrene thin films for spectroelectrochemical sensing, *Anal. Chem.* **81** (2009) 6756-6764.
83. Fehse K., Walzer K., Leo K., Lövenich W., Elschner A., Highly conductive polymer anodes as replacements for inorganic materials in high-efficiency organic light-emitting diodes, *Adv. Mater.* **19** (2007) 441-444.

84. Chen J., Asano M., Maekawa Y., Yoshida M., Suitability of some fluoropolymers used as base films for preparation of polymer electrolyte fuel cell membranes, *J. Membr. Sci.* **277** (2006) 249-257.
85. Kreuer K.D., Schuster M., Obliers B., Diat O., Traub U., Fuchs A., Klock U., Paddison S.J., Maier J., Short-side-chain proton conducting perfluorosulfonic acid ionomers: Why they perform better in PEM fuel cells, *J. Power Sources* **178** (2008) 499-509.
86. Makowski H.S., Lundberg R.D., Singhal G.H., Flexible polymeric compositions comprising a normally plastic polymer sulfonated to about 0.2 to about 10 mole % sulfonate, US Patent 3,870,841 (1975).
87. Hietala S., Holmberg S., Näsman J., Ostrovskii D., Paronen M., Serimaa R., Sundholm F., Torell L., Torkkeli M., The state of water in styrene-grafted and sulfonated poly(vinylidene fluoride) membranes, *Angew. Makromol. Chem.* **253** (1997) 151-167.
88. Lu Z., Polizo G., Macdonald D.D., Manias E., State of water in perfluorosulfonic ionomer (Nafion 117) proton exchange membranes, *J. Electrochem. Soc.* **155** (2008) B163-B171.
89. Ding F.C., Wang S.J., Xiao M., Meng Y.Z., Cross-linked sulfonated poly(phthalazinone ether ketone)s for PEM fuel cell application as proton-exchange membrane, *J. Power Sources* **164** (2007) 488-495.
90. Kaur S., Florio G., Michalak D., Cross-linking of sulfonated styrene-ethylene/butylene-styrene triblock polymer via sulfonamide linkages, *Polymer* **43** (2002) 5163-5167.
91. Gomes D., Buder I., Nunes S.P., Novel proton conductive membranes containing sulfonated silica, *Desalination* **199** (2006) 274-276.
92. Wang L., Xing D.M., Zhang H.M., Yu H.M., Liu Y.H., Yi B.L., MWCNTs reinforced Nafion® membrane prepared by a novel solution-cast method for PEMFC, *J. Power Sources* **176** (2008) 270-275.
93. Silva A.L.A., Takase I., Pereira R.P., Rocco A.M., Poly(styrene-co-acrylonitrile) based proton conductive membranes, *Eur. Polym. J.* **44** (2008) 1462-1474.
94. Rubatat L., Li C., Dietsch H., Nykänen A., Ruokolainen J., Mezzenga R., Structure-properties relationship in proton conductive sulfonated polystyrene-polymethyl methacrylate block copolymers (sPS-PMMA), *Macromolecules* **41** (2008) 8130-8137.
95. Navarro A., del Río C., Acosta J.L., Kinetic study of the sulfonation of hydrogenated styrene butadiene block copolymer (HSBS): Microstructural and electrical characterizations, *J. Membr. Sci.* **300** (2007) 79-87.
96. Kim J., Kim B., Jung B., Proton conductivities and methanol permeabilities of membranes made from partially sulfonated polystyrene-block-poly(ethylene-ran-butylene)-block-polystyrene copolymers, *J. Membr. Sci.* **207** (2002) 129-137.

97. Sangeetha D., Conductivity and solvent uptake of proton exchange membrane based on polystyrene(ethylene-butylene)polystyrene triblock polymer, *Eur. Polym. J.* **41** (2005) 2644-2652.
98. Mani S., Weiss R.A., Williams C.E., Hahn S.F., Microstructure of ionomers based on sulfonated block copolymers of polystyrene and poly(ethylene-*alt*-propylene), *Macromolecules* **32** (1999) 3663-3670.
99. Park M.J., Downing K.H., Jackson A., Gomez E.D., Minor A.M., Cookson D., Weber A.Z., Balsara N.P., Increased water retention in polymer electrolyte membranes at elevated temperatures assisted by capillary condensation, *Nano Lett.* **7** (2007) 3547-3552.
100. Mokrini A., Huneault M.A., Shi Z., Xie Z., Holdcroft S., Non-fluorinated proton-exchange membranes based on melt extruded SEBS/HDPE blends, *J. Membr. Sci.* **325** (2008) 749-757.
101. Piboonsatsanasakul P., Wootthikanokkhan J., Thanawan S., Preparation and characterizations of direct methanol fuel cell membrane from sulfonated polystyrene/poly(vinylidene fluoride) blend compatibilized with poly(styrene)-*b*-poly(methyl methacrylate) block copolymer, *J. Appl. Polym. Sci.* **107** (2008) 1325-1336.
102. Funck A., Kaminsky W., Polypropylene carbon nanotube composites by in situ polymerization, *Compos. Sci. Technol.* **67** (2007) 906-915.
103. Pötschke P., Pegel S., Claes M., Bonduel D., A Novel strategy to incorporate carbon nanotubes into thermoplastic matrices, *Macromol. Rapid Commun.* **29** (2008) 244-251.
104. Grossiord N., Kivit P.J.J., Loos J., Meuldijk J., Kyrylyuk A.V., van der Schoot P., Koning C.E., On the influence of the processing conditions on the performance of electrically conductive carbon nanotube/polymer nanocomposites, *Polymer* **49** (2008) 2866-2872.
105. Odian G., *Principles of polymerization*, 4th ed., John Wiley & Sons, New York, 2004, 812 pp.
106. Lovell A.P., El-Aasser M.S., editors, *Emulsion polymerization and emulsion polymers*, John Wiley and Sons, Chichester, 1997, 801 pp.
107. Zhang R., Guo L., Zhang M., Wen H., Zhao D., Chen Q., Gao G., Liu F., Emulsion polymerization of styrene and acrylic acid in the presence of carbon black, *Polym. Prepr.* **45** (2004) 1036-1037.
108. Jia Z., Wang Z., Xu C., Liang J., Wei B., Wu D., Zhu S., Study on poly(methyl methacrylate)/carbon nanotube composites, *Mater. Sci. Eng. A* **271** (1999) 395-400.
109. Park S.J., Cho M.S., Lim S.T., Choi H.J., Jhon M.S., Synthesis and dispersion characteristics of multi-walled carbon nanotube composites with poly(methyl methacrylate) prepared by in-situ bulk polymerization, *Macromol. Rapid Commun.* **24** (2003) 1070-1073.
110. Coleman J.N., Cadek M., Ryan K.P., Fonseca A., Nagy J.B., Blau W.J., Ferreira M.S., Reinforcement of polymers with carbon nanotubes. The role

of an ordered polymer interfacial region. Experiment and modeling, *Polymer* **47** (2006) 8556-8561.

111. Logakis E., Pandis C., Peoglos V., Pissis P., Stergiou C., Pionteck J., Pötschke P., Mičušík M., Omastová M., Structure-property relationships in polyamide 6/multi-walled carbon nanotubes nanocomposites, *J. Polym. Sci., Part B: Polym. Phys.* **47** (2009) 764-774.

112. Zhao C., Hu G., Justice R., Schaefer D.W., Zhang S., Yang M., Han C.C., Synthesis and characterization of multi-walled carbon nanotubes reinforced polyamide 6 via in situ polymerization, *Polymer* **46** (2005) 5125-5132.

113. Long Y., Chen Z., Wang N., Li J., Wan M., Electronic transport in PANI-CSA/PANI-DBSA polyblends, *Phys. B* **344** (2004) 82-87.

114. Davies S.J., Ryan T.G., Wilde C.J., Beyer G., Processable forms of conductive polyaniline, *Synth. Met.* **69** (1995) 209-210.

115. Datta S., Lohse D.J., *Polymeric compatibilizers*, Hanser Gardner Publications, Munich, 1996, 542 pp.

116. Domenech S.C., Bortoluzzi J.H., Soldi V., Franco C.V., Electroactive mixtures of polyaniline and EPDM rubber: Chemical, thermal, and morphological characterization, *J. Appl. Polym. Sci.* **87** (2003) 535-547.

117. Del Castillo-Castro T., Castillo-Ortega M.M., Herrera-Franco P.J., Rodríguez-Félix D.E., Compatibilization of polyethylene/polyaniline blends with polyethylene-graft-maleic anhydride, *J. Appl. Polym. Sci.* **119** (2011) 2895-2901.

118. Zheng W., Levon K., Taka T., Laakso J., Österholm J.-E., Phase behaviors and interactions of N-alkylated polyanilines and ethylene-co-vinyl acetate blends, *J. Polym. Sci., Part B: Polym. Phys.* **33** (1995) 1289-1306.

119. Zhang Q., Wang X., Geng Y., Chen D., Jing X., Morphology and thermal properties of conductive polyaniline/polyamide composite films, *J. Polym. Sci., Part A: Polym. Chem.* **40** (2002) 2531-2538.

120. Juvin P., Hasik M., Fraysse J., Planès J., Pron A., Kulszewicz-Bajer I., Conductive blends of polyaniline with plasticized poly(methyl methacrylate), *J. Appl. Polym. Sci.* **74** (1999) 471-479.

121. Zilberman M., Siegmann A., Narkis M., Melt-processed, electrically conductive ternary polymer blends containing polyaniline, *J. Macromol. Sci., Part B: Phys.* **39** (2000) 333-347.

122. Wan-Cheng L.K.P., Shacklette L.W., Han C., Intrinsically conductive polymer blends having a low percolation threshold, US Patent 5,908,898 (1999).

123. Zhang Q., Wang X., Chen D., Jing X., Electrically conductive, melt-processed ternary blends of polyaniline/dodecylbenzene sulfonic acid, ethylene/vinyl acetate, and low-density polyethylene, *J. Polym. Sci., Part B: Polym. Phys.* **42** (2004) 3750-3758.

124. Scheirs J., Kaminsky W., editors, *Metallocene-based polyolefins: preparation, properties and technology*, Vol. 1, John Wiley & Sons, Chichester, 2001, 526 pp.
125. Anttila U., Hakala K., Helaja T., Löfgren B., Seppälä J., Compatibilization of polyethylene/polyamide 6 blends with functionalized polyethylenes prepared with metallocene catalyst, *J. Polym. Sci., Part A: Polym. Chem.* **37** (1999) 3099-3108.
126. Paavola S., Uotila R., Löfgren B., Seppälä J.V., Enhanced adhesive properties of polypropylene through copolymerization with 10-undecen-1-ol, *React. Funct. Polym.* **61** (2004) 53-62.
127. Barra G.M.O., Leyva M.E., Soares B.G., Mattoso L.H., Sens M., Electrically conductive, melt-processed polyaniline/EVA blends, *J. Appl. Polym. Sci.* **82** (2001) 114-123.
128. Gwee L., Choi J., Winey K.I., Elabd Y.A., Block copolymer/ionic liquid films: The effect of ionic liquid composition on morphology and ion conduction, *Polymer* **51** (2010) 5516-5524.
129. Sernetz F.G., Mülhaupt R., Waymouth R.M., Influence of polymerization conditions on the copolymerization of styrene with ethylene using $\text{Me}_2\text{Si}(\text{Me}_4\text{Cp})(N\text{-tert-butyl})\text{TiCl}_2$ /methylaluminoxane Ziegler-Natta catalysts, *Macromol. Chem. Phys.* **197** (1996) 1071-1083.
130. Xu G., Lin S., Titanocene-methylaluminoxane catalysts for copolymerization of styrene and ethylene: Synthesis and characterization of styrene-ethylene copolymers, *Macromolecules* **30** (1997) 685-693.
131. Xu G., Copolymerization of ethylene with styrene catalyzed by the $[\eta^1:\eta^5\text{-tert-butyl}(\text{dimethylfluorenylsilyl})\text{amido}]methyltitanium$ "cation", *Macromolecules* **31** (1998) 2395-2402.
132. Sernetz F.G., Mülhaupt R., Amor F., Eberle T., Okuda J., Copolymerization of ethene with styrene using different methylalumoxane activated half-sandwich complexes, *J. Polym. Sci., Part A: Polym. Chem.* **35** (1997) 1571-1578.
133. Kallio T., Lundström M., Sundholm G., Walsby N., Sundholm F., Electrochemical characterization of radiation-grafted ion-exchange membranes based on different matrix polymers, *J. Appl. Electrochem.* **32** (2002) 11-18.



ISBN 978-952-60-4780-5
ISBN 978-952-60-4781-2 (pdf)
ISSN-L 1799-4934
ISSN 1799-4934
ISSN 1799-4942 (pdf)

Aalto University
School of Chemical Technology
Department of Biotechnology and Chemical Technology
www.aalto.fi

**BUSINESS +
ECONOMY**

**ART +
DESIGN +
ARCHITECTURE**

**SCIENCE +
TECHNOLOGY**

CROSSOVER

**DOCTORAL
DISSERTATIONS**